Modelling PM2.5 during severe atmospheric pollution episode in Lagos, Nigeria: Spatiotemporal variations, source apportionment, and meteorological influences

Ishaq Dimeji Sulaymon[1], Yuanxun Zhang[2], Philip K. Hopke[3], Fei Ye[4], Kangjia Gong[1], Jianjiong Mao[4], and Jianlin Hu[1]

[1]Nanjing University of Information Science and Technology
[2]University of Chinese Academy of Sciences
[3]University of Rochester
[4]Nanjing University of Information Science & Technology

December 20, 2022

Abstract

In 2021, the World Health Organization (WHO) ranked Nigeria among the most polluted nations in the world, an indication of a deteriorating air quality, especially in the major urban areas of the country, which might pose adverse human health impacts. In this study, the Integrated Source Apportionment Method (ISAM) tool in the Community Multiscale Air Quality (CMAQ) model (CMAQ-ISAM) was employed to quantify the contributions of eight emissions sectors to fine particulate matter (PM2.5) and its major components in Lagos during a prolonged severe atmospheric pollution episode (APE) in January 2021. The influence of meteorological conditions on the formation and dispersion of PM2.5 during the APE was also elucidated. Spatially, elevated PM2.5 concentrations were found in the northwestern region of Lagos, an urban area with larger anthropogenic emissions. Residential and industry were the two major sources of PM2.5. Residential contributed the most to total PM2.5 (~40 µg/m3), followed by industry (~20 µg/m3). High concentrations of secondary inorganic aerosols (SIA) at the northwest and upper northern areas of Lagos were majorly attributed to residential and industry sectors. In addition, sulfate accounted for the largest fraction of PM2.5, with residential, industry, and energy being its major sources. Residential, industry, and on-road sectors dominated the contributions to nitrate, while residential and industry were the major contributors to ammonium. Furthermore, the elevated PM2.5 concentrations during the APE were greatly enhanced by unfavorable meteorological conditions. This study provides insights for designing effective emissions control strategies to mitigate future severe PM2.5 pollution episode in Lagos.

Hosted file

951837_0_art_1_rmwwws.docx available at https://authorea.com/users/567852/articles/613985-modelling-pm2-5-during-severe-atmospheric-pollution-episode-in-lagos-nigeria-spatiotemporal-variations-source-apportionment-and-meteorological-influences

Modelling $PM_{2.5}$ during severe atmospheric pollution episode in Lagos, Nigeria: Spatiotemporal variations, source apportionment, and meteorological influences

Ishaq Dimeji Sulaymon[a*], Yuanxun Zhang[b,c], Philip K. Hopke[d,e], Fei Ye[a], Kangjia Gong[a], Jianjiong Mao[a], Jianlin Hu[a*]

[a] *Jiangsu Key Laboratory of Atmospheric Environment Monitoring and Pollution Control, Collaborative Innovation Center of Atmospheric Environment and Equipment Technology, School of Environmental Science and Engineering, Nanjing University of Information Science & Technology, Nanjing, 210044, China*

[b] *College of Resources and Environment, University of Chinese Academy of Sciences, Beijing 100049, China*

[c] *CAS Center for Excellence in Regional Atmospheric Environment, Chinese Academy of Sciences, Xiamen, 361021, China*

[d] *Center for Air Resources Engineering and Science, Clarkson University, Potsdam, NY 13699, USA*

[e] *Department of Public Health Sciences, University of Rochester School of Medicine and Dentistry, Rochester, NY 14642, USA*

[*] Corresponding author. *E-mail address:* sulaymondimeji@nuist.edu.cn; jianlinhu@nuist.edu.cn

Key Points:

- Lagos experienced a prolonged severe $PM_{2.5}$ pollution episode in January 2021.
- $PM_{2.5}$ pollution was enhanced by unfavorable meteorological conditions.
- Effective emissions control strategies to reduce $PM_{2.5}$ concentrations are urgently required in Lagos.

Abstract

In 2021, the World Health Organization (WHO) ranked Nigeria among the most polluted nations in the world, an indication of a deteriorating air quality, especially in the major urban areas of the country, which might pose adverse human health impacts. In this study, the Integrated Source Apportionment Method (ISAM) tool in the Community Multiscale Air Quality (CMAQ) model (CMAQ-ISAM) was employed to quantify the contributions of eight emissions sectors to fine particulate matter ($PM_{2.5}$) and its major components in Lagos during a prolonged severe atmospheric pollution episode (APE) in January 2021. The influence of meteorological conditions on the formation and dispersion of $PM_{2.5}$ during the APE was also elucidated. Spatially, elevated $PM_{2.5}$ concentrations were found in the northwestern region of Lagos, an urban area with larger anthropogenic emissions. Residential and industry were the two major sources of $PM_{2.5}$. Residential contributed the most to total $PM_{2.5}$ (~40 $\mu g/m^3$), followed by industry (~20 $\mu g/m^3$). High concentrations of secondary inorganic aerosols (SIA) at the northwest and upper northern areas of Lagos were majorly attributed to residential and industry sectors. In addition, sulfate accounted for the largest fraction of $PM_{2.5}$, with residential, industry, and energy being its major sources. Residential, industry, and on-road sectors dominated the contributions to nitrate, while residential and industry were the major contributors to ammonium. Furthermore, the elevated $PM_{2.5}$ concentrations during the APE were greatly enhanced by unfavorable meteorological conditions. This study provides insights for designing effective emissions control strategies to mitigate future severe $PM_{2.5}$ pollution episode in Lagos.

Keywords: Fine particulate matter; Source apportionment; CMAQ-ISAM; Atmospheric pollution episode; Residential emissions; Meteorological influences.

1. Introduction

Due to rapid population growth, accelerated urbanization, economic advancement, and fast industrialization, Nigeria has been suffering from severe air pollution for more than two decades (Abiye et al., 2013, 2014; Owoade et al., 2013; Sulaymon et al., 2020). In 2021, the WHO ranked Nigeria among the most polluted nations in the world (WHO, 2021), making it a great concern for the Nigerian air quality experts. The anthropogenic and natural emissions are the major sources of particulate matter and gaseous primary air pollutants (Owoade et al., 2013). Air pollution is largely linked to emissions from anthropogenic activities (either local or regional) (Sulaymon et al., 2020, 2021a) and aggravated by unfavorable meteorological factors (Hua et al., 2021; Hu et al., 2016; Sulaymon et al., 2021a, 2021b). Severe air pollution is strongly correlated with visibility reductions (Jiang et al., 2021; Li et al., 2019; Wang et al., 2018), changes in ecosystem services, effects on climate (Jiang et al., 2021; Zhao et al., 2021), acid rain (Owoade et al., 2021), and very serious human health impacts (Croft et al., 2019; Hopke et al., 2019; Shen et al., 2020; Yan et al., 2018), such as pneumonia, acute respiratory disorders, breathing problems, and chronic asthma (Rizwan et al., 2013). The global burden of disease project (GDB, 2020) has estimated that about 4.2 million premature deaths per annum around the globe are the result of exposure to air pollution.

Meteorological factors play major roles in the formation, accumulation, and dispersion of air pollutants (Hu et al., 2016; Islam et al., 2015; Mao et al., 2022; Okimiji et al., 2021; Owoade et al., 2021; Sulaymon et al., 2021a, 2021b, 2021c). Previous studies have posited that the atmospheric pollution dispersion is greatly influenced by relative humidity (RH), wind speed (WS), and planetary boundary layer height (PBLH)

(Li et al., 2019; Liu et al., 2017; Zhang et al., 2019; Zhang et al., 2018), and that low WS and PBLH hinder atmospheric pollutant dispersion and consequently lead to severe air pollution episodes (Dai et al., 2020; Li et al., 2019; Liu et al., 2017; Sulaymon et al., 2021a; Wang et al., 2020; Zhang et al., 2019).

Prior to January 2021, there were no ambient air quality monitoring networks in any of Nigerian cities. The lack of ambient data meant that the temporal and spatial variations of the major air pollutants (gaseous pollutants and particulate matter and its components) were unknown. Thus, studies to investigate the air quality and support development of effective pollution control strategies and reduce associated human health risks were very limited (Kitagawa et al., 2022; Hu et al., 2016). However, the problems associated with the air quality assessment in countries/regions with no or limited monitoring networks could be overcome through the use of source-tracking chemical transport models (CTMs) (Kitagawa et al., 2022). CTMs can simulate air pollutants with high resolution of temporal and spatial distributions (Kota et al., 2018), give hourly averaged gridded concentrations (Kitagawa et al., 2022), be used for source apportionment studies (Appel et al., 2020; Li et al., 2021; Ma et al., 2021; Shi et al., 2017), employed in human exposure assessment to air pollution (Guo et al., 2019; Reis et al., 2018), as well as utilized in epidemiological studies to unravel the adverse effects of air pollution on population (Andreão et al., 2020). CTMs have been extensively used in many parts of the world, such as North America (Guo et al., 2018; Hu et al., 2015a; Pan et al., 2017; Ying and Kleeman, 2006; Wang et al., 2021a; Ying et al., 2015; Zhang et al., 2013, 2014), China (Hu et al., 2015b, 2016, 2017; Gong et al., 2021; Ma et al., 2021; Qiao et al., 2015, 2019; Sulaymon et al., 2021a, 2021b; Wang et al., 2020; Ying et al., 2014), India (Guo et al., 2017, 2019; Guttikunda and Jawahar, 2014; Kota et al., 2014, 2018; Marrapu et al., 2014; Ye et al., 2022), South America (Albuquerque et al., 2018, 2019; Kitagawa et al., 2021, 2022; Nedbor-Gross et al., 2018; Pedruzzi et al., 2019, 2022), and Africa (Kumar et al., 2022; Marais et al., 2014, 2019).

With a population of about 23.5 million as at 2018, Lagos is the largest metropolitan city in Africa, and also the most economically and industrially-developed city in Nigeria. As a result, the city has been suffering from severe fine particulate matter ($PM_{2.5}$) pollution for more than two decades. To design effective emissions control strategies towards abating $PM_{2.5}$ pollution in any region, it is imperative to elucidate the contributions of various emissions sectors to $PM_{2.5}$ and its major components, as well as the meteorological influences over the region. The present work represents the first study that utilized the source-tracking Community Multiscale Air Quality (CMAQ) model to quantify the contributions of different emissions sectors to $PM_{2.5}$ and its major compositions in Lagos during a prolonged severe atmospheric pollution episode (APE) in January 2021. The capability and fidelity of the CMAQ model in simulating $PM_{2.5}$ in Lagos was validated by comparing the predicted concentrations with observation data, and the spatiotemporal distributions of $PM_{2.5}$ during the APE period were analyzed. In addition, the impacts of meteorological conditions on $PM_{2.5}$ during the APE were elucidated. This study provides insights into the emissions sectors dominating $PM_{2.5}$ pollution in Lagos and the meteorological influences, and the results could serve as scientific basis for formulating cost-effective emissions control strategies towards mitigating $PM_{2.5}$ pollution in Lagos and the surrounding regions.

2. Methodology

2.1. Model configurations

The Community Multiscale Air Quality version 5.3.2 (CMAQv5.3.2) model was employed to simulate the air quality in Lagos, Nigeria. The required meteorological fields for the CMAQ model were simulated using the Weather Research and Forecasting (WRF) model version 4.0. The initial and boundary conditions (IC/BC) of WRF model were based on the dataset of NCEP FNL (Final) Operational Model Global Tropospheric Analysis. The major physics schemes are listed in Table S1. Further detailed settings and configurations of WRF model adopted in this study can be found in previous studies (Hu et al., 2015b, 2016; Wang et al., 2021b). In this study, the simulations were conducted in two domains using one-way nesting approach (Fig. 1). Domain 1 covers the entire Nigeria with a horizontal resolution of 36 km x 36 km (137 x 107 grids). Domain 2 mostly covers Lagos and surrounding areas at with a horizontal resolution of 12 km x 12 km (127 x 202 grids). The model was configured with the State-wide Air Pollution Research Center version 07 (SAPRC07tic) photochemical mechanism and the AERO6i aerosol module (Sulaymon et al., 202Ia, 2021b). Details about the vertical resolution of the two CMAQ domains have been described in Sulaymon et al. (2021b). The simulation period was January 2021, during which two severe APEs occurred. The IC/BC of Domain 1 simulation were generated using the default profiles provided by the CMAQ model. The IC/BC used for the 12 km domain simulation were estimated based on the results of the nested simulation. To minimize the effects of initial conditions on the model predictions, the simulation started five days ahead of the simulation period, hence, regarded as the spin-up period (Tao et al., 2020).

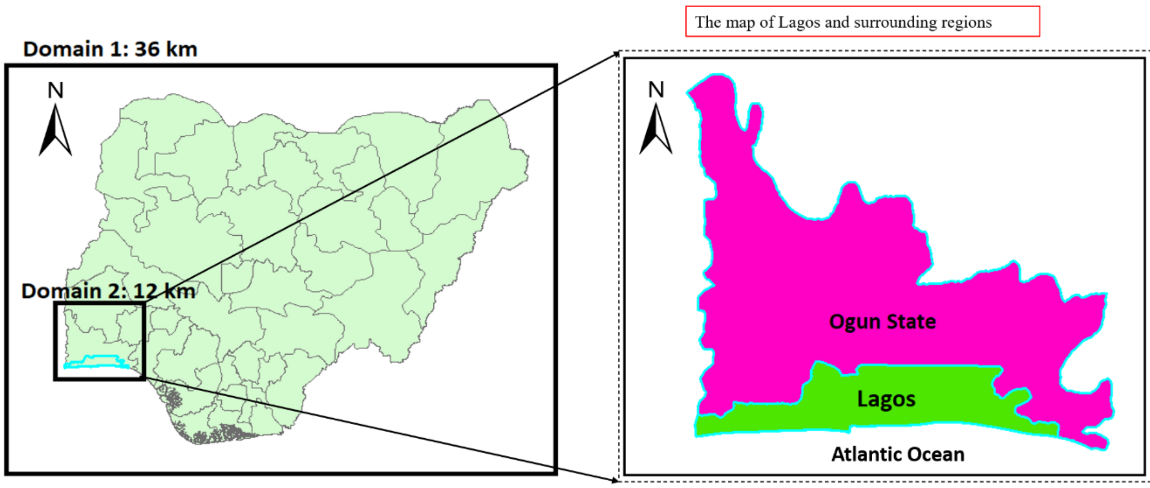

Fig. 1. The WRF-CMAQ simulation domains used in this study (left) and the map of Lagos and surrounding regions (right).

2.2. Emissions inventory

In this study, the Integrated Source Apportionment Model (ISAM), a source tracking tool in the CMAQ model, was applied to quantify the source contributions to $PM_{2.5}$ and its major components (Jiang et al., 2021; Kwok et al., 2013; Li et al., 2021) in Lagos. The anthropogenic emissions used in this study were derived from the Emissions Database for Global Atmospheric Research version 5.0 (EDGARv5.0) (Crippa et al., 2020). The EDGAR emissions inventory includes the annual emissions of carbon monoxide (CO), nitrogen oxides (NO_X), sulfur dioxide (SO_2), ammonia (NH_3), non-methane volatile organic compounds (NMVOCs), $PM_{2.5}$, particulate matter with an aerodynamic diameter less than 10 μm (PM_{10}), elemental carbon (EC), and organic carbon (OC) from various emissions sectors and with a spatial resolution of 0.1° x 0.1°. The emissions sectors were subsequently classified into six categories (agriculture, residential, industry, energy, on-road transportation, and off-road transportation). It is worthy to mention that the EDGAR emissions inventory had been used in numerous previous studies in India (Guo et al., 2019, 2018, 2017; Kota et al., 2018), China (Qiao et al., 2019), and Africa as a continent (Kumar et al., 2022; Mazzeo et al., 2022). In addition, biogenic emissions were estimated with the Model of Emissions of Gases and Aerosols from Nature (MEGAN) version 2.1 (Guenther et al., 2012). Also, open burning emissions were generated based on the data obtained from the Fire Inventory from NCAR (FINN) (Wiedinmyer et al., 2011). Furthermore, sea salt and windblown emissions were generated inline (Sulaymon et al., 2021a, 2021b). Overall, a total of eight emission sectors were tracked in the ISAM model. Further details regarding the emission processing can be found in Qiao et al. (2019).

3. Results and discussion

3.1. WRF model performance

Previous studies have elucidated the crucial roles of meteorological factors in the formation, transportation, as well as dissipation of fine particulate matter and other air pollutants (Hua et al., 2021; Hu et al., 2016; Sulaymon, et al., 2021a, 2021d). Therefore, in assuring the accuracy of air quality simulations, a robust and satisfactory WRF model performance must be obtained. In evaluating the performance of WRF model, the simulated temperature (T2) and relative humidity (RH) at 2 m above surface, and wind speeds (WS) and wind directions (WD) at 10 m above ground level were compared with observation data downloaded from the official website of the National Climate Data Center (NCDC) (ftp://ftp.ncdc.noaa.gov/pub/data/noaa/, last accessed on October 30, 2022). The temporal variations of the meteorological variables and $PM_{2.5}$ are illustrated in Fig. 2. Table 1 provides the statistical indices, including the mean observation (OBS), mean prediction (PRE), mean bias (MB), mean error (ME), and the root mean square error (RMSE). With MB and ME values of 0.24 and 0.60, respectively, which fell below the suggested

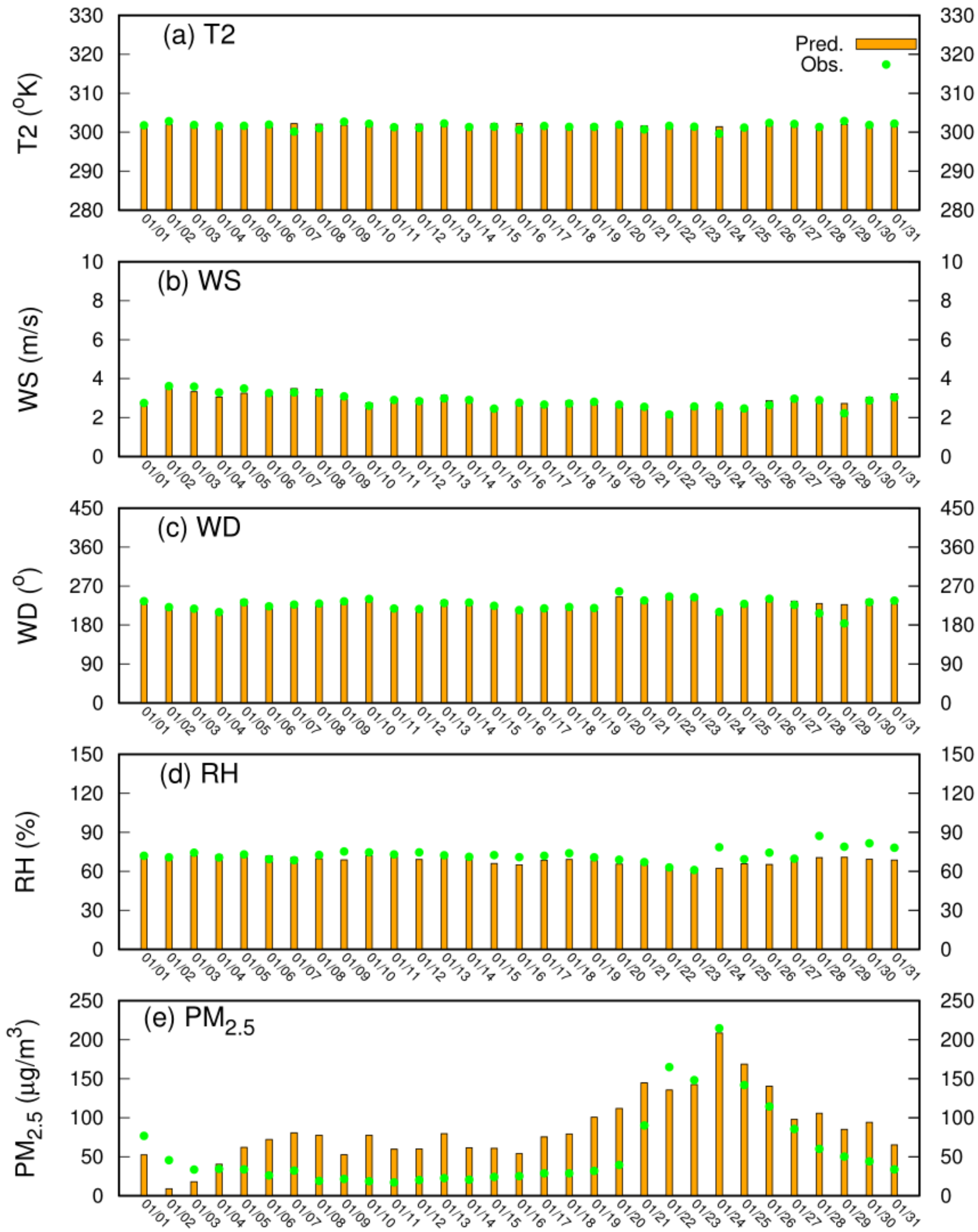

Fig. 2. Temporal variations of the predicted and observed meteorological variables (temperature, wind speed, wind direction, and relative humidity) and $PM_{2.5}$ concentrations in Lagos during January 2021.

benchmarks (MB≤ ±0.5; ME≤2.0) (Emery et al., 2001), T2 (Fig. 2a) was well-reproduced by the WRF model. Similar statistical indices and model performance of T2 had been reported in the Beijing-Tianjin-Hebei (BTH) region of China during winter (January 2014) (Lang et al., 2021). Wind speed was slightly over-estimated during the study period, however, considering the fact that its MB, ME, and RMSE indices were far below the suggested benchmarks (Table 1), the WRF model in this study showed a better performance in capturing the observed WS as illustrated in Fig. 2(b).

Table 1. Model performance of meteorological factors in Lagos, Nigeria (OBS: observed mean; PRE: predicted mean; MB: mean bias; ME: mean error; RMSE: root mean square error).

	Metrics	January	Benchmarks
T2 (K)	OBS	301.6	
	PRE	301.8	
	MB	0.24	≤±0.5
	ME	0.6	≤2.0
	RMSE	0.78	
WS (m/s)	OBS	2.87	
	PRE	2.90	
	MB	0.03	≤±0.5
	ME	0.14	≤2.0
	RMSE	0.17	≤2.0
WD (°)	OBS	226.3	
	PRE	228.5	
	MB	2.17	≤±10
	ME	5.69	≤±30
	RMSE	9.90	
RH (%)	OBS	72.6	
	PRE	68.6	
	MB	-4.04	
	ME	4.55	
	RMSE	6.21	

The over-estimation of WS might be due to unresolved topography in the WRF model (Li et al., 2014). The statistical indices (MB and ME) of WS in this study are consistent with those reported by Lang et al. (2021) and Sulaymon et al. (2021b). As illustrated in Fig. 2(c), the predominant WD during the study period was southwesterly. Similar to T2 and WS, WD was also over-predicted during the simulation period. However, the predicted WD showed better agreement with observations, having found both MB and ME indices falling below the suggested benchmarks (MB≤±10; ME≤±30). Similar model performance had been reported by Ma et al. (2021) and Qiao et al. (2019). Relative humidity (Fig. 2d) was underpredicted with MB and ME values of -4.04 and 4.55, respectively. Although, there are presently no performance benchmarks for RH. Previous studies in India (Bhati and Mohan, 2018), China (Hu et al., 2016; Li et al., 2021; Sulaymon et al., 2021a, 2021b), and Brazil (Kitagawa et al., 2021; Pedruzzi et al., 2021) had also reported under-estimation of RH. Bhati and Mohan (2018) had linked under-estimation of RH to the influence of boundary layer parameterization on meteorological prediction. Generally, the WRF model performances in the present study were satisfactory and better when compared to previous studies from other parts of the world (Bhati and Mohan, 2018; Hu et al., 2016; Kitagawa et al., 2021; Kota et al., 2018; Pedruzzi et al., 2021; Sulaymon et al., 2021a; Yu et al., 2021). Since the WRF model has shown a robust and better performance in this study, the meteorological fields were utilized in driving the air quality simulation.

3.2. CMAQ model performance

To evaluate the performance of the CMAQ model in reproducing the observed $PM_{2.5}$ in Lagos, the model was evaluated based on some statistical indices, including the mean observations (OBS), mean predictions (PRE), mean fractional bias (MFB), mean fractional error (MFE), mean normalized bias (MNB), and mean normalized error (MNE). The hourly $PM_{2.5}$ observation data were downloaded from the official website of the United States of America (USA) Embassy, Lagos (https://www.airnow.gov/international/us-embassies-and-consulates/#Nigeria$Lagos, last accessed on October 30, 2022). Necessary quality checks were carried out on the data before being used for evaluation (Sulaymon et al., 2021c). The CMAQ model performances in predicting $PM_{2.5}$ during January 2021 in Lagos are illustrated in Table 2. The observed $PM_{2.5}$ concentration was well-simulated in Lagos, with the model performance indices falling within the recommended benchmarks (MFB $\leq\pm0.60$; MFE $\leq$ 0.75) (Boylan and Russel, 2006). The temporal variations of the observed and simulated $PM_{2.5}$ concentrations are illustrated in Fig. 2(e). With positive MFB (0.52), the CMAQ model over-predicted $PM_{2.5}$ concentrations during the study period. Overall, the CMAQ model in this study has exhibited a good performance when compared to previous studies around the world (Jiang et al., 2021; Kitagawa et al., 2021; Kota et al., 2018; Mao et al., 2022; Pedruzzi et al., 2021; Sulaymon et al., 2021a; Tao et al., 2020). Therefore, the predicted $PM_{2.5}$ concentrations were deemed acceptable for further analyses.

Table 2. Model performance of $PM_{2.5}$ in Lagos, Nigeria (OBS: observed average; PRE: predicted average; MFB: mean fractional bias; MFE: mean fractional error; MNB: mean normalized bias; MNE: mean normalized error). The study period was January 2021. The performance benchmarks for $PM_{2.5}$ were suggested by Boylan and Russell (2006).

	Metrics	January	Benchmarks
$PM_{2.5}$ ($\mu g/m^3$)	OBS	56.4	
	PRE	86.2	
	MFB	0.52	$\leq\pm0.60$
	MFE	0.69	≤0.75
	MNB	1.09	
	MNE	1.21	

3.3. Statistical analysis of $PM_{2.5}$ during different pollution levels

As illustrated in Fig. 2 (e), it can be observed that throughout the simulation period (except on January 2 and 3), the 24-hr total $PM_{2.5}$ concentrations in Lagos greatly exceeded the old daily air quality guideline (AQG) level (25 μg/m^3) recommended by the World Health Organization (WHO, 2005). Furthermore, considering the new WHO AQG level (15 μg/m^3) (WHO, 2021) for $PM_{2.5}$, only one day (January 2 with $PM_{2.5}$ value of 11.92 μg/m^3) could be described as a clean day, while the remaining days witnessed different levels of $PM_{2.5}$ pollution, ranging from slight to severe pollution. Based on the daily $PM_{2.5}$ concentrations, air quality can be grouped into various pollution levels. In this study, the $PM_{2.5}$ pollution levels were categorized into five groups (Table S2). Table S3 shows the statistical results of $PM_{2.5}$ in January based on different pollution levels. Under clean level, the simulated $PM_{2.5}$ concentrations were below the old WHO AQG level. However, the simulated maximum $PM_{2.5}$ concentration exceeded the new AQG value of WHO, indicating that even during the clean days, exposure to $PM_{2.5}$ at low levels could still cause adverse effects to human health. Under the slightly-polluted level, there were 12 days with concentration range of $35 \leq PM_{2.5} < 75$. The simulated minimum, maximum, and mean $PM_{2.5}$ greatly breached the old and new AQG levels of WHO. For instance, the simulated mean $PM_{2.5}$ was 2.5 and 4.2 times the old and new AQG level, respectively. Considering the moderately-polluted level (10 days with concentration range of 75≤ $PM_{2.5}$<115), it could be noted that the simulated mean $PM_{2.5}$ was 3.7 and 6.2 times the old and new AQG level, respectively. Under the heavily-polluted level, the simulated mean $PM_{2.5}$ was 5.4 and 9.1 times the old and new AQG level, respectively. The simulated $PM_{2.5}$ ranged between 167.3-198.6 μg/m^3, with mean of 182.9 μg/m^3. $PM_{2.5}$ under the heavily-polluted level greatly exceeded the old and new AQG levels by 7.3 and 12.2 times, respectively. The results of this study showed that the residents of Lagos were greatly exposed to high $PM_{2.5}$ pollution throughout January 2021, and this could lead to adverse human health effects (Croft et al., 2019; Hopke et al., 2019; Shen et al., 2020; Yan et al., 2018).

3.4. Spatial variations of $PM_{2.5}$ and its major components during the pollution episode

The spatial distributions of the simulated $PM_{2.5}$ concentrations and its major components during the study period are illustrated in Fig. 3. An atmospheric pollution episode (APE) is said to occur when daily $PM_{2.5}$ concentration persistently exceeds 50 μg/m^3 (interim target 2 of WHO) (WHO, 2021) for at least two consecutive days (Sulaymon et al., 2021b; Zhang et al., 2019). An APE occurred in January 2021, and was characterized with high $PM_{2.5}$ concentrations. The APE (50 μg/m^3 ≤ $PM_{2.5}$) lasted for 27 days (January 5-31). Spatially, highest $PM_{2.5}$ concentrations ($PM_{2.5}$ ≥ 120 μg/m^3) were noted in the northwestern region of Lagos metropolis, while the rest of the city was characterized with 60 ≤ $PM_{2.5}$ ≤ 120 μg/m^3. During the prolonged pollution episode, the averaged city-wide concentration was 94.6 μg/m^3, while $PM_{2.5}$ concentrations in the northwest were as high as 150-220 μg/m^3. This indicates the severity of $PM_{2.5}$ pollution during the APE.

Among the three components that make the secondary inorganic aerosols (SIA), sulfate (SO_4^{2-}) had the highest contributions, followed by ammonium (NH_4^+), and nitrate (NO_3^-). Sulfate was evenly distributed across the city, with higher concentrations (6-15 μg/m^3) located in the northwestern and upper northern areas. For ammonium, higher concentrations (2-3 μg/m^3) were found in the upper north and northwest areas, while other areas were concentrated with 0.8-2 μg/m^3 of NH_4^+. Similar to sulfate and ammonium, nitrate also peaked in the northwest area. It can be deduced that among the three SIA species, sulfate contributed most to $PM_{2.5}$.

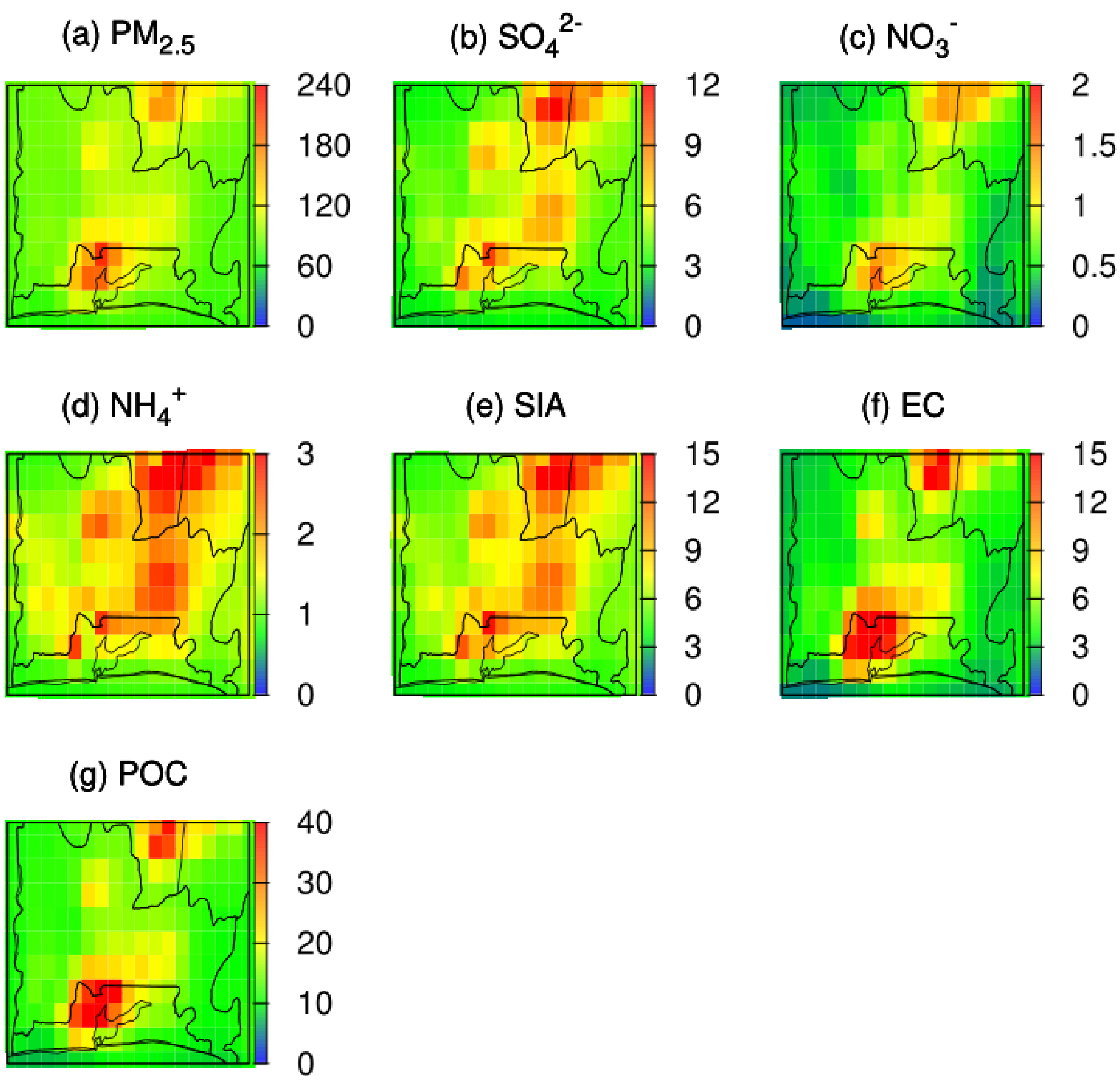

Fig. 3. Spatial distributions of the predicted total $PM_{2.5}$ and its major components in Lagos during the atmospheric pollution episode. Units are μg/m^3.

Overall, SIA (sum of SO_4^{2-}, NO_3^-, and NH_4^+) was evenly distributed over Lagos, with higher concentrations (6-15 μg/m^3) located in the northwestern, northern, and central areas. In addition, during the pollution episode, the concentrations of elemental carbon (EC) and primary organic carbon (POC) were notably very high in the northwestern area of Lagos. The northwestern area (which includes Ikeja, Agege, Ifako-Ijaye, Oshodi, Mushin, Shomolu, Surulere, and Ajegunle areas) is densely populated and highly industrialized (Owoade et al., 2013), which results to high energy consumption. In addition, the Muritala Muhammed International Airport (MMIA), which is the busiest and largest international airport in Nigeria and West Africa, is located in the northwestern part of Lagos. Generally, Lagos is characterized with heavy daily traffic (Okimiji et al., 2021; Owoade et al., 2013), especially in the early morning and late afternoon (the local rush hours). The northwestern region records more traffic than any other region. High traffic volumes can be attributed to the presence of the administrative offices of several governmental agencies as well as those of many private enterprises. Therefore, emissions from local anthropogenic sources particularly in the northwestern region of the city are likely the dominant contributors to the elevated $PM_{2.5}$ concentrations. However, polluted winds being transported from the neighboring cities in Ogun State, which borders Lagos in the north could also aggravate the $PM_{2.5}$ pollution, especially in the northwestern area of Lagos.

3.5. Spatiotemporal variations of $PM_{2.5}$ during the pollution episode

Fig. 4 shows the daily spatial variations of the predicted $PM_{2.5}$ during the APE in Lagos and its neighboring cities. Except in the northwestern area of Lagos, $PM_{2.5}$

concentrations in most parts of the city were less than 100 μg/m^3 during the first 14 days of the episode (January 5-18). This could be attributed to elevated PBLH during the period (Fig. S1), since high PBLH values lead to reduced pollution level (Tao et al., 2020). The higher PBLH were generally noted within Lagos metropolis and its surroundings during January 5-18. Within Lagos, the PBLH ranged between 200 and 850 m, with an average regional value of 560 m. In the northwestern region, however, a very intense pollution episode was observed throughout the period (January 5-18), with 100 μg/m^3 being the

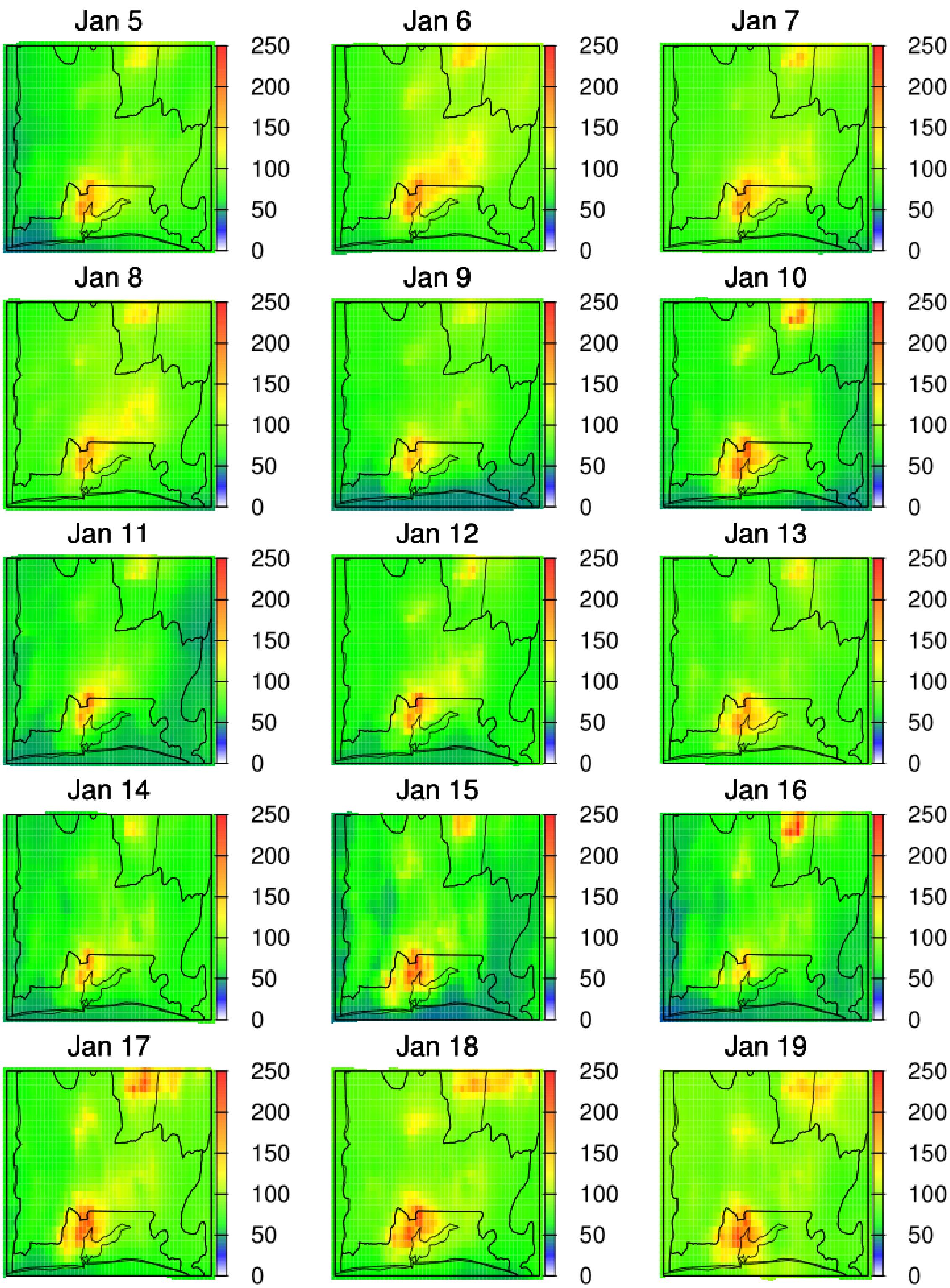

Fig. 4. Spatial distributions of the predicted total $PM_{2.5}$ concentrations in Lagos during the atmospheric pollution episode. Units are $\mu g/m^3$.

minimum regional daily $PM_{2.5}$ concentration. As stated in section 3.4, the northwestern region of Lagos is an urban area with several chemical industries and heavy traffic. Thus, it is a major hub of anthropogenic emissions. During the first four days (January 5-8) of the episode, high wind speeds (3-6 m/s) were observed in most of Lagos metropolis, especially in the northwestern and central areas (Fig. S2). The APE began on January 5 (Fig. 4) with high haze ($50 \leq PM_{2.5} \leq 120$ μg/m^3) noted across the major parts of the study area except at the northwestern area where a cluster of very high pollution ($150 \leq PM_{2.5} < 200$ μg/m^3) was found. Prior to the inception of the city-wide heavy haze on January 6, a high $PM_{2.5}$ pollution cluster was initially noted in the northwestern area on January 5 (Fig. 4). On January 6, a strong northwesterly wind (Fig. S2) enhanced the transportation of pollutants to other parts of the Lagos metropolis. Due to the continuous flow of the northwesterly winds, the $PM_{2.5}$ pollution cluster that was initially formed in the northwestern area on January 5, steadily got spread to and enveloped the entire study area, with regional $PM_{2.5}$ concentrations exceeding 100 μg/m^3 on January 6 (Fig. 4). This trend persisted until January 8. On several days (e.g January 9 and 11), the pollution was low ($PM_{2.5} \leq 50$ μg/m^3) in most areas of Lagos (except the northern and central areas), especially in the western and eastern parts of the city. With different pollution intensities across Lagos and its surrounding cities, the APE continued till January 31. As previously discussed and illustrated in Fig. 4, there were tendencies of cross-regional transport of $PM_{2.5}$ pollution from the surrounding cities (bordering Lagos to the north) into the study area. The transported pollution could have aggravated the pollution level generally caused by local anthropogenic emissions. Compared to January 16 (with moderate pollution), higher pollution was noted across the Lagos metropolis on January 17 and 18, with the highest being found in the northwestern area of the city.

Compared to the first 14 days, the $PM_{2.5}$ concentrations across Lagos metropolis and specifically in the northwestern area were relatively higher during the last 13 days of the episode (January 19-31) (Fig. 4). During this period (January 19-31), the wind speed in most of Lagos ranged between 2-4 m/s (Fig. S2), with the lowest values being observed in the northwestern area. The lack of dispersion could have driven the severe haze recorded in the northwestern region as lower wind speed reduces the dispersion of pollutants (Sulaymon et al, 2021a). Generally, the PBLH within Lagos metropolis was lower during January 19-30 compared to January 5-18. During January 19-30 of the APE, the daily averaged PBLH was between 150-800 m, having an average regional value of 491 m. Generally, the formation of high $PM_{2.5}$ pollution is enhanced by low PBLH and WS (Li et al., 2019; Sulaymon et al, 2021a; Tao et al., 2020; Wang et al., 2020). For instance, on January 19, a high $PM_{2.5}$ concentration was noted in northwestern Lagos (Fig. 4). Due to the stagnant and low wind speeds (especially during January 19-25) across the Lagos metropolis and specifically in the northwestern region, the APE persisted until January 31. The pollution episode became more significant on January 21, with average regional $PM_{2.5}$ reaching 120 $\mu g/m^3$, while the concentrations in the northwestern region exceeded 200 $\mu g/m^3$. The severe pollution continued until January 24 when it peaked with the $PM_{2.5}$ concentrations above 150 $\mu g/m^3$ widely spread across the Lagos metropolis and its surrounding cities in the north. The highest concentrations ($PM_{2.5}$>200 $\mu g/m^3$) were not only found in the northwestern but also in the southwestern and southern parts of Lagos nearest to the ocean. On January 25, severe haze was still recorded in the northwestern and southern parts of Lagos, although lower than January 24. The other areas had $PM_{2.5}$

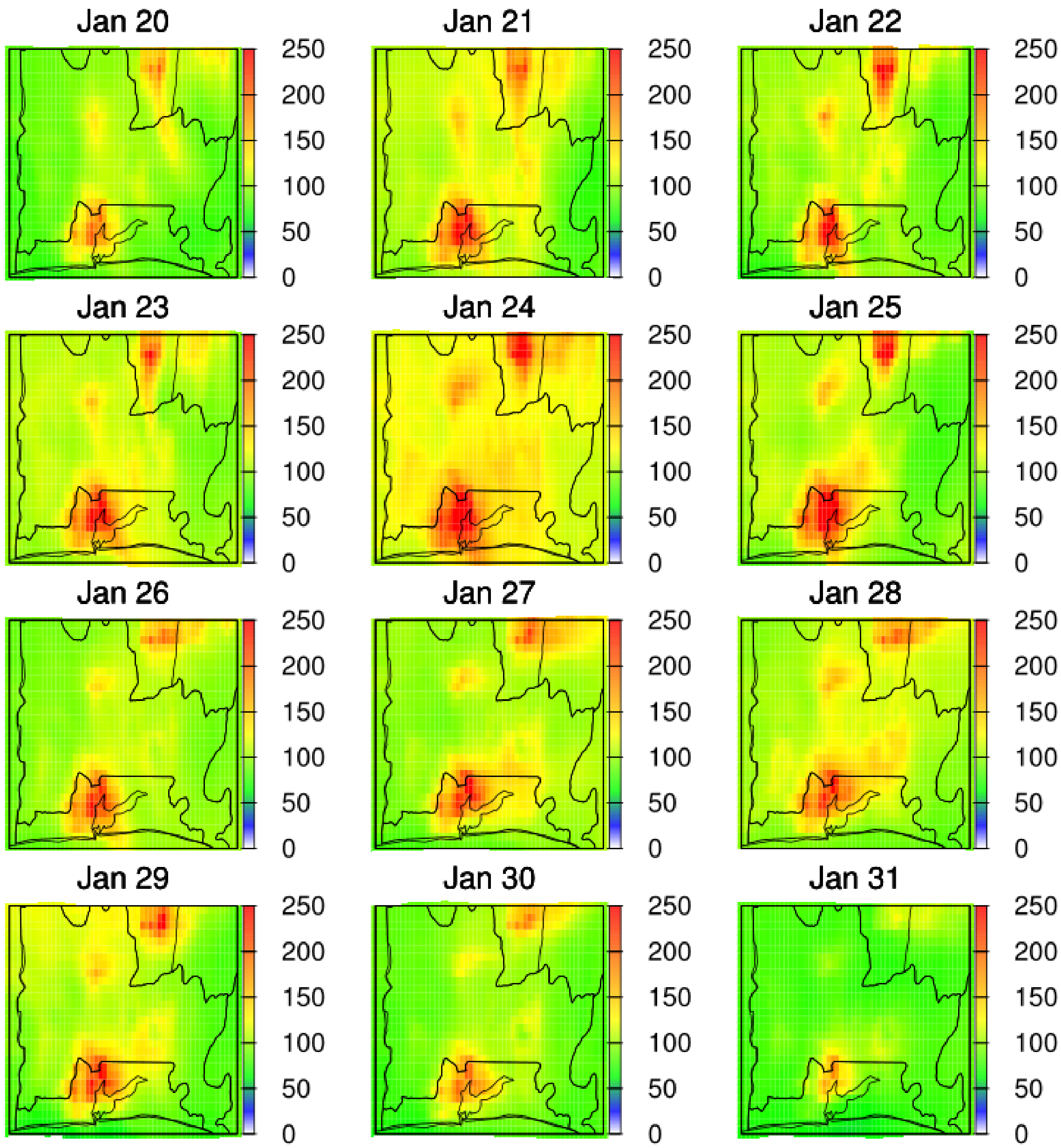

Fig. 4. (continued).

concentrations ranging between 60 and 120 μg/m^3, and the haze persisted until January 31 when the APE ended with a decline to moderate to high regional pollution. With 27 days characterized with high $PM_{2.5}$ concentrations during the episode, Lagos was subjected to severe $PM_{2.5}$ pollution during January 2021. Therefore, quantifying the contributions from each emission sector to total $PM_{2.5}$ and its major components during the APE became highly imperative, as the results would provide scientific basis for designing and implementing effective emission control strategies towards abating $PM_{2.5}$ pollution in the city.

3.6. Source apportionment of $PM_{2.5}$ and its major components

The temporal variations of the contributions of different sources to daily $PM_{2.5}$ and its major components in Lagos during the APE are illustrated in Fig. 5. During the study period, the averaged contributions of residential, industry, open burning, and IC/BC to total $PM_{2.5}$ (Fig. 5a) in Lagos were 36.2, 16.5, 0.78, and 3.57 μg/m^3, respectively. The three major sources of EC (Fig. 5b) were residential, industry, and ICBC, with averaged contributions of 18.9, 4.46, and 1.00 μg/m^3, respectively. Following the same arrangement of the sources for EC, the contributions of the sectors towards SO_4^{2-} (Fig. 5c) were 3.71, 1.43, and 1.25 μg/m^3, respectively. In addition to the three major sources of SO_4^{2-}, there were also slight contributions from energy and open burning sectors on most of the days of the episode. For NH_4^+ (Fig. 5d), residential and industry were the dominant sectors with averaged contributions of 1.04 and 0.27 μg/m^3, respectively. The contributions from on-road transport, off-road transport, energy, agriculture, and biogenic sectors to $PM_{2.5}$, EC, and NH_4^+ were very low. Considering NO_3^- (Fig. 5e), all of the emission sectors contributed towards its daily formation, with residential, industry, and on-road serving as the three major contributors. It should be noted that the contributions of residential and industry sectors were generally higher during the last 13 days of the episode than the first 14 days of the episode.

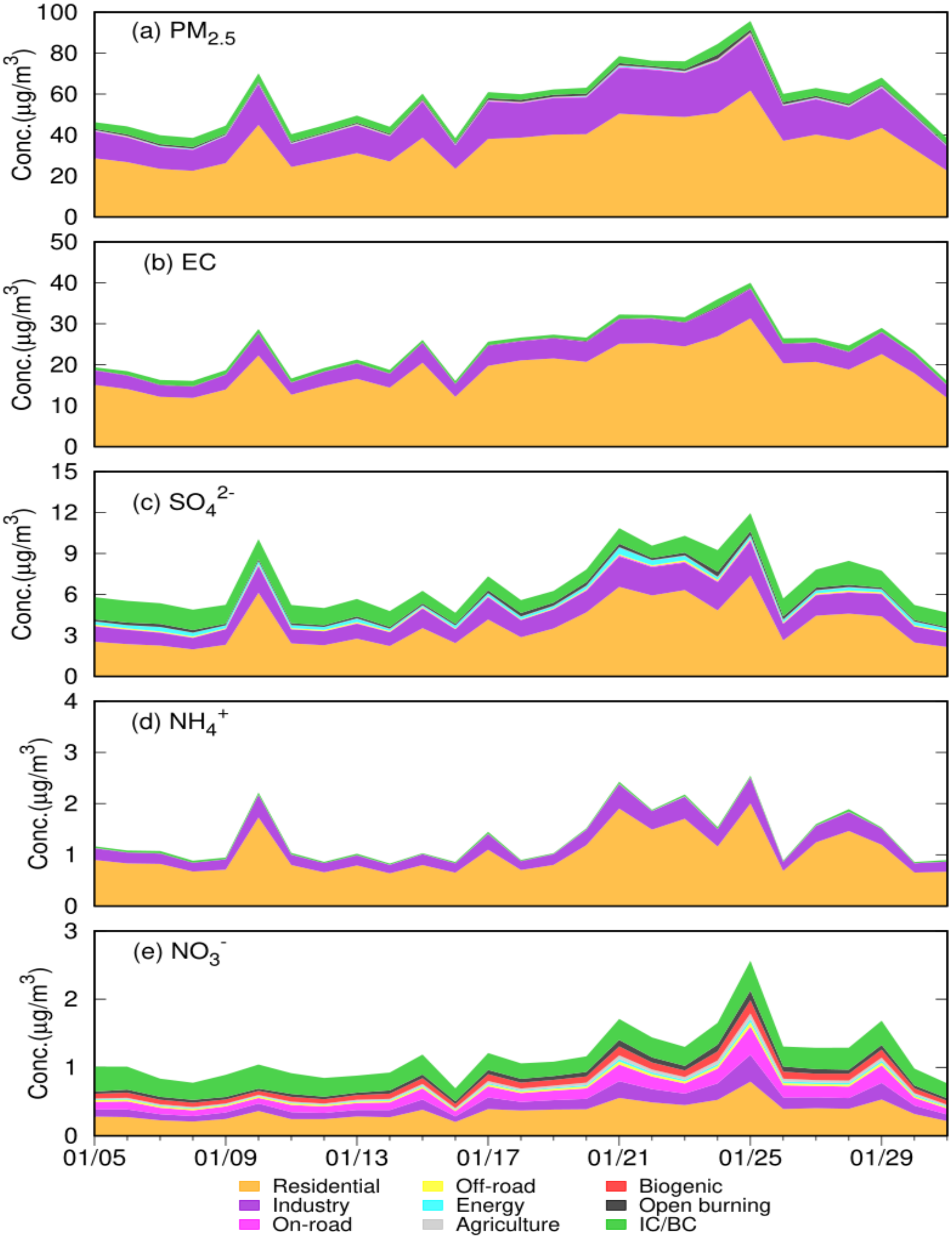

Fig. 5. Daily contributions of emissions sectors to the predicted (a) total $PM_{2.5}$, (b) EC, (c) SO_4^{2-}, (d) NH_4^+, and (e) NO_3^- during the atmospheric pollution episode.

Fig. 6 illustrates the spatial distributions of various source contributions to the averaged total $PM_{2.5}$ in Lagos during the episode. High contributions from residential (20-40 μg/m^3) and industry (10-20 μg/m^3) were found in the northwestern area of the city. In other areas of Lagos, the contributions of residential and industrial emissions were up to 20 μg/m^3 and 10 μg/m^3, respectively. This is consistent with the results of Guo et al. (2017).

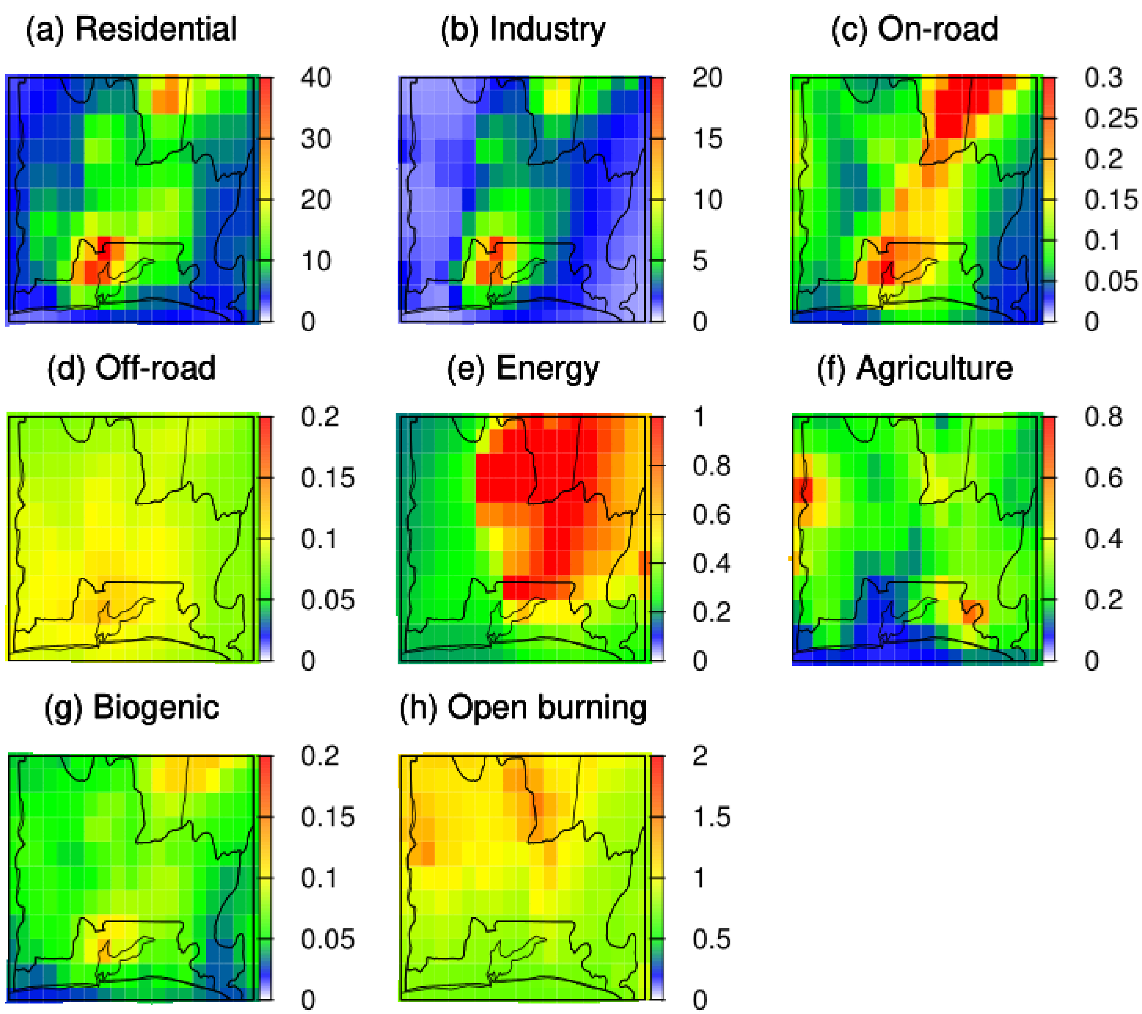

Fig. 6. Source apportionment of total $PM_{2.5}$ from (a) residential, (b) industry, (c) on-road, (d) off-road, (e) energy, (f) agriculture, (g) biogenic, and (h) open burning during the atmospheric pollution episode. Units are μg/m^3.

Guo et al. (2017) had previously used EDGAR emissions inventory in a source-oriented CMAQ model for the source apportionment of $PM_{2.5}$ in North India, and found residential emissions as the highest contributor, followed by industrial sector. In addition, the elevated $PM_{2.5}$ concentrations in major Chinese cities during winter period had been linked to residential burning for heating purposes, industrial emissions, construction activities, and road dust (Guo et al., 2020). $PM_{2.5}$ contributed by open burning was up to 1 μg/m^3, and uniformly distributed across the city. Energy also contributed up to 1 μg/m^3, especially in the upper northern areas The contributions from other emissions sectors to $PM_{2.5}$ during the pollution episode were low (less than 1 μg/m^3) across the city.

The percentage contributions of emission sectors to $PM_{2.5}$ and its major components during the APE are shown in Fig. 7, with residential and industrial sectors dominating. The contributions of residential to $PM_{2.5}$, EC, SO_4^{2-}, and NH_4^+ were 66.7, 80.3, 65.3, and 79.1%, respectively, while the industry contributed 30.4, 19.0, 25.1, and 20.4% to $PM_{2.5}$, EC, SO_4^{2-}, and NH_4^+, respectively. Energy and open burning also notably contributed to SO_4^{2-}, with 4.0 and 3.1%, respectively. For NO_3^-, the contributions of residential, industry, on-road, biogenic, open burning, agriculture, off-road, and energy were 41.3, 16.8, 16.8, 10.0, 6.5, 3.4, 3.3, and 2.0%, respectively. These findings are consistent with the results of Zhao et al. (2021), where industrial and residential sectors were the major contributors to $PM_{2.5}$ in six cities of East-central China during the COVID-19 lockdown. The dominance of residential sector could be attributed to the cooking activities by the dense population of Lagos residents, while the dominance of industrial sector could be associated with emissions from large-scale industries in the city. Also, Li et al. (2020) and Ma et al. (2021) had reported residential and industrial sectors as the dominant contributors to $PM_{2.5}$ in YRD region, China. Furthermore, residential and industry were the major emission sectors contributing to $PM_{2.5}$ in the BTH region of China, especially during winter season (Chang et al., 2019).

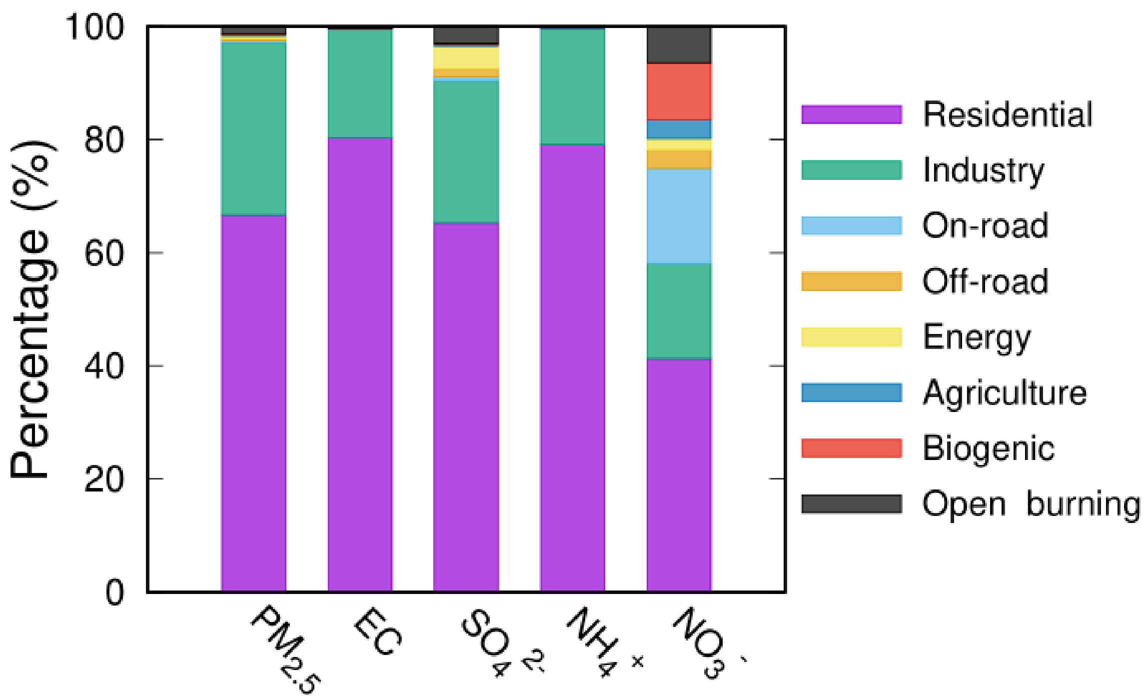

Fig. 7. Contributions of different emissions sectors to total $PM_{2.5}$ and its major components during the atmospheric pollution episode.

3.7. Source apportionment of secondary inorganic aerosols (SIA)

Previous studies have identified the secondary inorganic aerosols (sulfate, nitrate, and ammonium) as the major components of total $PM_{2.5}$ (Guo et al., 2017; Li et al., 2021; Shi et al., 2017). The contributions of different emissions sectors to SIA are shown in Fig. 8, while the source contributions to SO_4^{2-}, NO_3^-, and NH_4^+ are illustrated in Figs S3, S4, and S5, respectively. Similar to $PM_{2.5}$, residential and industry served as the major emission sectors contributing to SIA. Considering the total contributions of all the emissions sectors to SIA during the APE (Fig. 8i), higher concentrations of SIA were majorly concentrated in the northwest, upper north, and central areas of Lagos, and were dominated by the contributions from residential (~9 μg/m^3) and industry (~3 μg/m^3) as illustrated in Figs 8(a) and 8(b), respectively, while other areas were filled with low but substantive SIA concentrations (3-6 μg/m^3) (Fig. 8i).

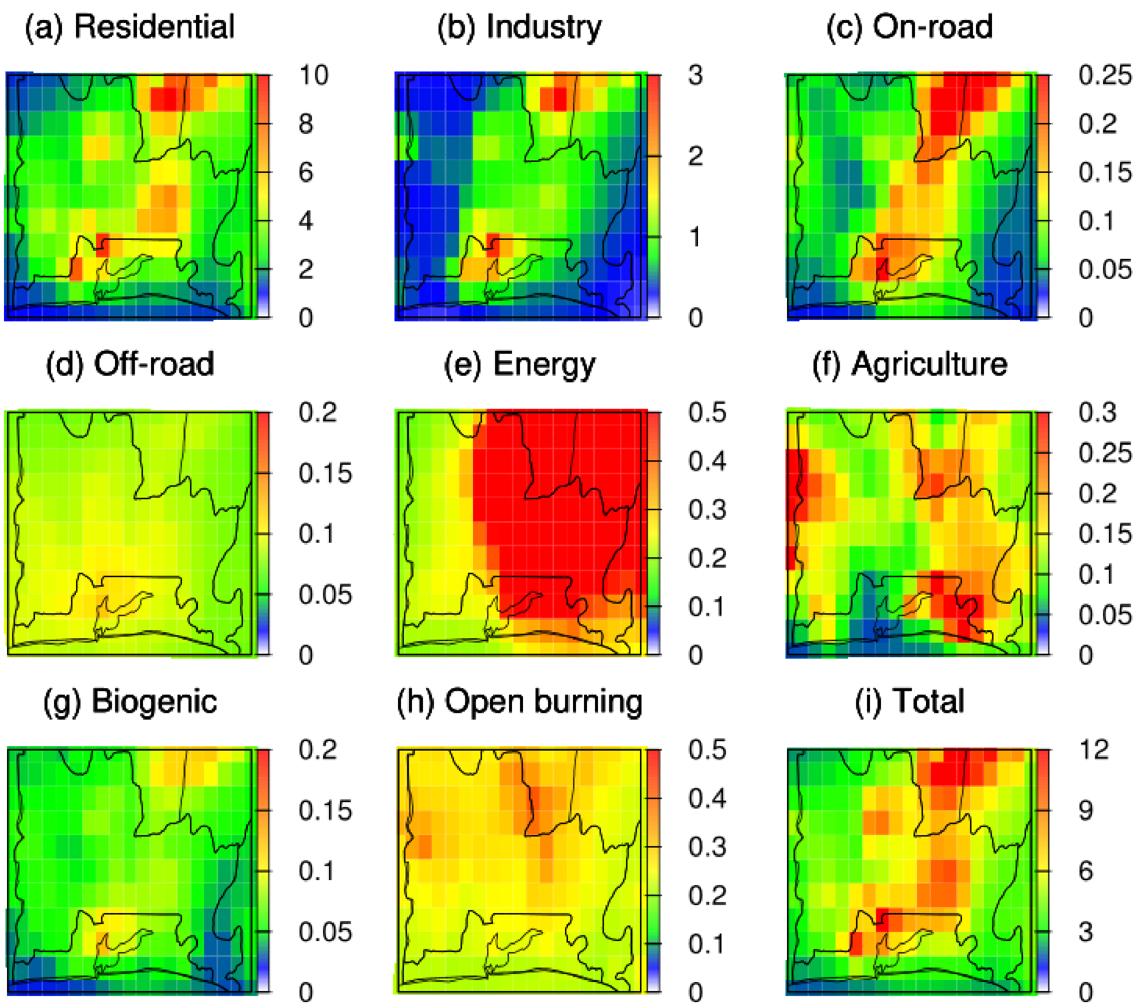

Fig. 8. Source apportionment of SIA from (a) residential, (b) industry, (c) on-road, (d) off-road, (e) energy, (f) agriculture, (g) biogenic, and (h) open burning during the atmospheric pollution episode. Units are μg/m^3.

High contributions from residential (2-9 μg/m^3) were located in the north and central areas of Lagos, while up to 3 μg/m^3 contributions due to industry were located in the northwest. The contributions from other emission sectors to SIA were very low. As shown in Fig. S3, residential and industry were the dominant sources of sulfate. Sulfate concentrations from residential (up to 6 μg/m^3) and industry (~2 μg/m^3) are concentrated in the north of Lagos (particularly the northwest), as the region is densely populated and highly industrialized. Residential, industry, and on-road transport sectors were the major sources of nitrate (Fig. S4). Furthermore, only residential and industry served as the major sectors contributing to NH_4^+ (Fig. S5). Just as the concentrations of $PM_{2.5}$ were higher during the APE, higher SIA concentrations were also noted during the study period. This reveals the severity of $PM_{2.5}$ pollution in Lagos during the pollution episode in January 2021. Overall, the substantive contributions of residential and industry sectors to $PM_{2.5}$ and SIA during the APE suggests that controlling residential and industrial emissions would pave way towards reducing $PM_{2.5}$ and its major components in Lagos.

3.8. Influence of meteorological factors on $PM_{2.5}$ pollution

Previous studies have revealed that meteorological factors such as high RH, low WS, and low PBLH hinder the dispersion of atmospheric pollutants, resulting into the formation of severe air pollution, especially during the cold season (Li et al., 2019; Liu et al., 2016; Sulaymon et al., 2021a; Wang et al., 2020; Zhang et al., 2019). As earlier discussed, low PBLH (Fig. S1) and WS (Fig. S2) were noted across Lagos during the study period. Therefore, the ventilation coefficient (VC) was used to evaluate the effectiveness of atmospheric dispersion during the APE period. VC (in m^2s^{-1}) was obtained as the product of WS and PBLH. Previous studies have widely employed VC in evaluating the efficiency of atmospheric dispersion of air pollutants (Dai et al., 2020; Sulaymon et al., 2021a; Tiwari et al., 2019), hence, further details about VC can be found in the referenced studies. The temporal variations of $PM_{2.5}$ and VC in Lagos during

January are illustrated in Fig. S6. As a result of poor dispersion, low VC values (<2000 m^2/s) were generally noted during the APE period, an indication of very high $PM_{2.5}$ pollution. During January 2-3 and 6-9, however, highest VC values were observed, indicating that the $PM_{2.5}$ pollution during those days was low compared to the last 15 days of the month (especially January 17-30). Low VC enhanced the accumulation of high $PM_{2.5}$ concentrations (Dai et al., 2020; Tiwari et al., 2019), which subsequently led to the prolonged high-pollution days during the study period, especially during January 17-30. For instance, the VC on January 2 (1844.1 m^2s^{-1}) was the highest, and it was approximately twice the VC on January 24 (1017.9 m^2s^{-1}), when the APE attained its peak. Correspondingly, the highest $PM_{2.5}$ concentration (208.7 $\mu g/m^3$) occurred on January 24, the same day with the lowest VC.

Furthermore, the influence of meteorological factors on $PM_{2.5}$ was assessed using the Pearson correlation analysis between $PM_{2.5}$ concentrations and four meteorological parameters (WS, PBLH, RH, and T2) during the APE. $PM_{2.5}$ was negatively correlated with WS (r^2=-0.535) and PBLH (r^2=-0.539). Zhang et al. (2019) had reported negative correlations between $PM_{2.5}$ and WS and PBLH. Sulaymon et al. (2021c, 2021d) and Zhang et al. (2015) also reported an inverse relationship between $PM_{2.5}$ and WS. In addition, the association between $PM_{2.5}$ and RH was negative (r^2=-0.456). The negative correlation found between RH and $PM_{2.5}$ in this study is consistent with those previously reported in Lagos (Okimiji et al., 2021), Wuhan (Sulaymon et al., 2021c), Dhaka (Islam et al., 2015), and Kathmandu (Giri et al., 2008). Negative correlations were also found between $PM_{2.5}$ and RH in Shanghai and Guangzhou (Zhang et al., 2015), especially during the winter period. Considering the relationship between $PM_{2.5}$ and temperature,

$PM_{2.5}$ also exhibited negative correlation with T2 (r^2=-0.347) during the APE, which is contrary to the findings of Okimiji et al. (2021) and Zhang et al. (2015) during winter. However, the inverse correlation found between T2 and $PM_{2.5}$ in this study is consistent with previous studies in Kathmandu (Giri et al., 2008) and Hefei and Suzhou (Sulaymon et al., 2021d), and was attributed to the cooling effect of particulate matter as a result of its negative radioactive forces (Islam et al., 2015). The results of this study also showed that the elevated $PM_{2.5}$ concentrations in Lagos during the APE were aggravated by unfavorable meteorological conditions. Therefore, when designing emission control strategies towards reducing the level of $PM_{2.5}$ in Lagos, it is very important to understand the crucial roles being played by both chemistry and meteorology in the formation, transportation, and dispersion of air pollutants as revealed in this study.

4. Conclusions

This study investigated the source apportionment of $PM_{2.5}$ and its major components in Lagos during a prolonged severe atmospheric pollution episode in January 2021, using the CMAQ-ISAM model. The influence of meteorological factors on $PM_{2.5}$ concentrations during the atmospheric pollution episode was also elucidated. The WRF model reasonably and well-simulated the meteorological fields (temperature, wind speed, wind direction, and relative humidity) for the CMAQ model, while the CMAQ model exhibited good performances in reproducing the observed $PM_{2.5}$ concentration during the simulation period. Spatially, elevated $PM_{2.5}$ concentrations were found in the northwestern region of Lagos, an urban area with larger anthropogenic emissions. The formation of elevated $PM_{2.5}$ during the APE was greatly enhanced by low WS and PBLH. The results of the ISAM showed that residential and industry sectors were the major contributors to $PM_{2.5}$ and SIA concentrations in Lagos during the APE. Residential and industry contributed about 40 μg/m^3 and 20 μg/m^3, respectively to total $PM_{2.5}$. SO_4^{2-} accounted for the largest fraction of $PM_{2.5}$, attaining 6.0 μg/m^3, with residential, industry, and energy being its major sources. Residential, industry, and on-road sectors dominated the contributions to NO_3^-, while residential and industry served as the major sources of NH_4^+. Also, this study improves the understanding of the mechanisms that resulted to the prolonged atmospheric pollution episode in Lagos under diverse meteorological influences. The results of this study reveal that the control of $PM_{2.5}$ pollution in Lagos is urgently required, and this could be achieved by substantially reducing the emissions from residential and industry sectors in Lagos and its neighboring cities.

Acknowledgements

This work was supported by the National Natural Science Foundation of China (42007187).

Conflict of Interest

The authors declare that they have no conflict of interest.

Open Research

The code for the CMAQ model could be obtained from the website of the United States Environmental Protection Agency (https://www.epa.gov/cmaq/access-cmaq-source-code, last access: October, 2022) and the code of WRF model is available on the WRF users' page (https://www2.mmm.ucar.edu/wrf/users/download/get_sources.html, last access: October, 2022). The Emissions Database for Global Atmospheric Research (EDGAR) can be found online (https://edgar.jrc.ec.europa.eu/dataset_ap50, last access: October, 2022). The Fire INventory from NCAR (FINN) can be download (https://www.acom.ucar.edu/Data/fire/, last access: October 2022). The meteorological observation is publicly available on the official website of the National Climate Data Center (NCDC) (ftp://ftp.ncdc.noaa.gov/pub/data/noaa/, last access: October 2022). The hourly $PM_{2.5}$ observation data can be downloaded online (https://www.airnow.gov/international/us-embassies-and-consulates/#Nigeria$Lagos, last access: October 2022). The simulated data ($PM_{2.5}$, its major components, and meteorological factors) and the observation data ($PM_{2.5}$ and meteorological factors) used for postprocessing (Figures and tables) in this study can be accessed online (https://doi.org/10.5281/zenodo.7409425). All of the figures were created by the Python Programming Language version 3.8 (https://www.python.org/downloads/, last access: October 2022).

References

Abiye, O.E., Obioh, I.B., and Ezeh, G.C.: Elemental characterization of urban particulates at receptor locations in Abuja, north-Central Nigeria. Atmos. Environ. 81, 695-701, 2013.

Abiye, O.E., Obioh, I.B., Ezeh, G.C., Alfa, A., Ojo, E.O., and Ganiyu, A.K.: Receptor modeling of atmospheric aerosols in Federal Capital Territory (FCT), Nigeria. IFE J.Sci. 16, 107-119, 2014.

Albuquerque, T.T. de A., Andrade, M.D.F., Ynoue, R.Y., Moreira, D.M., Andre˜ao, W.L., and Soares, F.: WRF-SMOKE-CMAQ Modeling System for Air Quality Evaluation in S˜ao Paulo Megacity with a 2008 Experimental Campaign Data, https://doi.org/10.1007/s11356-018-3583-9, 2018.

Albuquerque, T.T. de A., West, J., Andrade, M. de F., Ynoue, R., Andre˜ao, W.L., Santos, F. S. dos, Maciel, F.M., Pedruzzi, R., Mateus, V. de O., Martins, J.A., Martins, L.D., Nascimento, E.G.S., and Moreira, D.M.: Analysis of $PM_{2.5}$ concentrations under pollutant emission control strategies in the metropolitan area of S˜ao Paulo, Brazil. Environ. Sci. Pollut. Res. 26, 33216-33227, https://doi.org/10.1007/s11356-019- 06447-6, 2019.

Andreão, W.L., Pinto, J.A., Pedruzzi, R., Kumar, P., and Albuquerque, T.T.de A.: Quantifying the impact of particle matter on mortality and hospitalizations in four Brazilian metropolitan areas. J. Environ. Manage. 270, https://doi.org/10.1016/j.jenvman.2020.110840, 2020.

Appel, K.W., Bash, J., Fahey, K., Foley, K., Gilliam, R., Hogrefe, C., Hutzell, W., Kang, D., Mathur, R., Murphy, B., Napelenok, S., Nolte, C., Pleim, J., Pouliot, G., Pye, H., Ran, L., Roselle, S., Sarwar, G., Schwede, D., Sidi, F., Spero, T., and Wong, D.: The community multiscale air quality (CMAQ) model versions 5.3 and 5.3.1: system updates and evaluation. Geosci. Model Dev. Discuss. 1-41, https://doi.org/10.5194/gmd-2020-345, 2020.

Bhati, S. and Mohan, M.: WRF-urban canopy model evaluation for the assessment of heat island and thermal comfort over an urban airshed in India under varying land use/land cover conditions. Geoscience Letters, 5(1), https://doi.org/10.1186/s40562-018-0126-7, 2018.

Boylan, J. W. and Russel, A. G.: PM and light extinction model performance metrics, goals, and criteria for three-dimensional air quality models. Atmos. Environ., 40, 4946-4959, https://doi.org/10.1016/j.atmosenv.2005.09.087, 2006.

Chang, X., Wang, S., Zhao, B., Xing, J., Liu, X., Wei, L., Song, Y., Wu, W., Cai, S., Zheng, H., Ding, D., and Zheng, M.: Contributions of inter-city and regional transport to $PM_{2.5}$ concentrations in the Beijing-Tianjin-Hebei region and its implications on regional joint air pollution control. Science of the Total Environment, 660, 1191- 1200, https://doi.org/10.1016/j.scitotenv.2018.12.474, 2019.

Crippa, M., Solazzo, E., Huang, G., Guizzardi, D., Koffi, E., Muntean, M., Schieberle, C., Friedrich, R., and Janssens-Maenhout, G.: High resolution temporal profiles in the Emissions Database for Global Atmospheric Research. Scientific Data, 7(1), https://doi.org/10.1038/s41597-020-0462-2, 2020.

Croft, D. P., Zhang, W., Lin, S., Thurston, S. W., Hopke, P. K., Masiol, M., Squizzato, S., van Wijngaarden, E., Utell, M. J., and Rich, D. Q.: The association between respiratory infection and air pollution in the setting of air quality policy and economic change. Annals of the American Thoracic Society, 16(3), 321–330, https://doi.org/10.1513/AnnalsATS.201810-691OC, 2019

Dai, Q., Liu, B., Bi, X., Wu, J., Liang, D., Zhang, Y., Feng, Y., and Hopke, P. K: Dispersion normalized PMF provides insights into the significant changes in source contributions to $PM_{2.5}$ after the CoviD-19 outbreak. Environmental Science and Technology, 54(16), 9917-9927, https://doi.org/10.1021/acs.est.0c02776, 2020.

Emery, C., Liu, Z., Russell, A.G., Odman, M.T., Yarwood, G., and Kumar, N.: Recommendations on statistics and benchmarks to assess photochemical model performance. J. Air Waste Manag. Assoc. 67 (5), 582-598, https://doi.org/10.1080/10962247.2016.1265027, 2017.

Giri, D., Murthy, K.V., and Adhikary, P.R.: The Influence of Meteorological Conditions on PM10 Concentrations in Kathmandu Valley. Int. J. Environ. Res., 2, 49-60, 2008

Global Burden of Disease (GBD).: Global age-sex-specific fertility, mortality, healthy life expectancy (HALE), and population estimates in 204 countries and territories, 1950-2019: a comprehensive demographic analysis for the Global Burden of Disease Study 2019, Lancet 396: 1135-1159, 2020.

Gong, K., Li, L., Li, J., Qin, M., Wang, X., Ying, Q., Liao, H., Guo, S., Hu, M., Zhang, Y., and Hu, J.: Quantifying the Impacts of Inter-City Transport on Air Quality in the Yangtze River Delta Urban Agglomeration, China: Implications for Regional Cooperative Controls of $PM_{2.5}$ and O_3. Sci. Total Environ., 779, 146619, 2021.

Guenther, A. B., Jiang, X., Heald, C. L., Sakulyanontvittaya, T., Duhl, T., Emmons, L. K., and Wang, X.: The Model of Emissions of Gases and Aerosols from Nature version 2.1 (MEGAN2.1): An extended and updated framework for modeling biogenic emissions. Geosci. Model Dev, 5, 1471-1492, https://doi.org/10.5194/gmdd-5-1-2012, 2012.

Guo, D., Wang, R., and Zhao, P.: Spatial distribution and source contributions of $PM_{2.5}$ concentrations in Jincheng, China. Atmos. Pollut. Res., 11(8), 1281-1289, 10.1016/j.apr.2020.05.004, 2020.

Guo, H., Kota, S. H., Sahu, S. K., Hu, J., Ying, Q., Gao, A., and Zhang, H.: Source apportionment of $PM_{2.5}$ in North India using source-oriented air quality models. Environmental Pollution, 231, 426-436, https://doi.org/10.1016/j.envpol.2017.08.016, 2017.

Guo, H., Han, F., Wang, Z., Pardue, J., and Zhang, H.: Deposition of sulfur and nitrogen components in Louisiana in August, 2011. Sci. Tot. Environ., 636, 124-133, https://doi.org/10.1016/j.scitotenv.2018.04.258, 2018.

Guo, H., Kota, S. H., Sahu, S. K., and Zhang, H.: Contributions of local and regional sources to $PM_{2.5}$ and its health effects in north India. Atmos. Environ., 214, https://doi.org/10.1016/j.atmosenv.2019.116867, 2019.

Guttikunda, S.K. and Jawahar, P.: Atmospheric emissions and pollution from the coalfired thermal power plants in India. Atmos. Environ. 92, 449-460, 2014.

Hopke, P. K., Croft, D., Zhang, W., Lin, S., Masiol, M., Squizzato, S., Thurston, S. W., van Wijngaarden, E., Utell, M. J., and Rich, D. Q.: Changes in the acute response of respiratory diseases to $PM_{2.5}$ in New York State from 2005 to 2016. Science of the Total Environment, 677, 328-339, https://doi.org/10.1016/j.scitotenv.2019.04.357, 2019.

Hua, J., Zhang, Y., de Foy, B., Shang, J., Schauer, J. J., Mei, X., Sulaymon, I. D., and Han, T.: Quantitative estimation of meteorological impacts and the COVID-19 lockdown reductions on NO_2 and $PM_{2.5}$ over the Beijing area using Generalized Additive Models (GAM). Journal of Environmental Management, 291, https://doi.org/10.1016/j.jenvman.2021.112676, 2021.

Hu, J., Zhang, H., Ying, Q., Chen, S.H., Vandenberghe, F., and Kleeman, M.J.: Long-term particulate matter modeling for health effect studies in California – Part I: Model performance on temporal and spatial variations. Atmospheric Chemistry and Physics, 15, 3445-3461, https://doi.org/10.5194/acp-15-3445-2015, 2015a.

Hu, J., Wu, L., Zheng, B., Zhang, Q., He, K., Chang, Q., Li, X., Yang, F., Ying, Q., and Zhang, H.: Source contributions and regional transport of primary particulate matter in China. Environmental Pollution, 207, 31–42. https://doi.org/10.1016/j.envpol.2015.08.037, 2015b.

Hu, J., Chen, J., Ying, Q., and Zhang, H.: One-year simulation of ozone and particulate matter in China using WRF/CMAQ modeling system. Atmospheric Chemistry and Physics, 16(16), 10333–10350, https://doi.org/10.5194/acp-16-10333-2016, 2016.

Hu, J., Li, X., Huang, L., Ying, Q., Zhang, Q., Zhao, B., Wang, S., and Zhang, H.: Ensemble prediction of air quality using the WRF/CMAQ model system for health effect studies in China. Atmospheric Chemistry and Physics, 17, 13103-13118, https://doi.org/10.5194/acp-17-13103-2017, 2017.

Islam, M.M., Afrin, S., Ahmed, T., and Ali, M.A.: Meteorological and seasonal influences in ambient air quality parameters of Dhaka city. J. Civ. Eng., 43, 67-77, 2015.

Jiang, Y., Xing, J., Wang, S., Chang, X., Liu, S., Shi, A., Liu, B., and Sahu, S. K.: Understand the local and regional contributions on air pollution from the view of human health impacts. Frontiers of Environmental Science and Engineering, 15(5), https://doi.org/10.1007/s11783-020-1382-2, 2021.

Kitagawa, Y. K. L., Pedruzzi, R., Galvão, E. S., de Araujo, I, B., Alburquerque, T.T.A., Kumar, P., Nascimento, E. G. S., and Moreira, D. M.: Source apportionment modeling of $PM_{2.5}$ using CMAQ-ISAM over a tropical coastal-urban area. Atmos. Pollut. Res., 12, https://doi.org/10.1016/j.apr.2021.101250, 2021.

Kitagawa, Y. K. L., Kumar, P., Galvão, E. S., Santos, J. M., Reis, N. C., Nascimento, E. G. S., and Moreira, D. M.: Exposure and dose assessment of school children to air pollutants in a tropical coastal-urban area. Science of the Total Environment, 803, https://doi.org/10.1016/j.scitotenv.2021.149747, 2022.

Kota, S.H., Zhang, H., Chen, G., Schade, G.W., and Ying, Q.: Evaluation of on-road vehicle CO and NOx National Emission Inventories using an urban-scale source-oriented air quality model. Atmos. Environ. 85, 99-108, 2014.

Kota, S.H., Guo, H., Myllyvirta, L., Hu, J., Sahu, S.K., Garaga, R., Ying, Q., Gao, A., Dahiya, S., Wang, Y., and Zhang, H.: Year-long simulation of gaseous and particulate air pollutants in India. Atmos. Environ. 180, 244-255, 2018.

Kumar, R., He, C., Bhardwaj, P., Lacey, F., Buchholz, R. R., Brasseur, G. P., Joubert, W., Labuschagne, C., Kozlova, E., and Mkololo, T: Assessment of regional carbon monoxide simulations over Africa and insights into source attribution and regional transport. Atmos. Environ. 119075, https://doi.org/10.1016/j.atmosenv.2022.119075, 2022.

Kwok, R. H. F., Napelenok, S. L., and Baker, K. R.: Implementation and evaluation of $PM_{2.5}$ source contribution analysis in a photochemical model. Atmos. Environ. 80, 398-407, https://doi.org/10.1016/j.atmosenv.2013.08.017, 2013.

Lang, J.L., Liang, X., Li, S., Zhou, Y., Chen, D., Zhang, Y., and Xu, L.: Understanding the impact of vehicular emissions on air pollution from the perspective of regional transport: A case study of the Beijing-Tianjin-Hebei region in China. Science of the Total Environment, 785, https://doi.org/10.1016/j.scitotenv.2021.147304, 2021.

Li, M., Song, Y., Huang, X., Li, J., Mao, Y., Zhu, T., Cai, X., and Liu, B.: Improving mesoscale modeling using satellite-derived land surface parameters in the pearl river delta region, China. Journal of Geophysical Research, 119(11), 6325–6346, https://doi.org/10.1002/2014JD021871, 2014.

Li, M., Zhang, Z., Yao, Q., Wang, T., Xie, M., Li, S., Zhuang, B., and Han, Y.: Nonlinear responses of particulate nitrate to NOx emission controls in the megalopolises of China. Atmospheric Chemistry and Physics, 21(19), 15135–15152, https://doi.org/10.5194/acp-21-15135-2021, 2021.

Li, X., Huang, L., Li, J., Shi, Z., Wang, Y., Zhang, H., Ying, Q., Yu, X., Liao, H., and Hu, J.: Source contributions to poor atmospheric visibility in China. Resources, Conservation & Recycling, 143, 167-177, 2019.

Liu, J., Mauzerall, D. L., Chen, Q., Zhang, Q., Song, Y., Peng, W., Klimont, Z., Qiu, X. H., Zhang, S. Q., Hu, M., Lin, W. L., Smith, K. R., and Zhu, T.: Air pollutant emissions from Chinese households: A major and underappreciated ambient pollution source. P. Natl. Acad. Sci. USA, 113, 7756-7761, 2016.

Ma, J., Shen, J., Wang, P., Zhu, S., Wang, Y., Wang, P., Wang, G., Chen, J., and Zhang, H.: Modeled changes in source contributions of particulate matter during the COVID-19 pandemic in the Yangtze River Delta, China. Atmospheric Chemistry and Physics, 21(9), 7343-7355, https://doi.org/10.5194/acp-21-7343-2021, 2021.

Mao, J., Li, L., Li, J., Sulaymon, I.D., Xiong, K., Wang, K., Zhu, J., Chen, G., Ye, F., Zhang, N., Qin, Y., Qin, M., and Hu, J.: Evaluation of long-term modeling fine particulate matter and ozone in China during 2013-2019. Front. Environ. Sci. 10:872249, 10.3389/fenvs.2022.872249, 2022.

Marais, E. A., Jacob, D. J., Wecht, K., Lerot, C., Zhang, L., Yu, K., Kurosu, T. P., Chance, K., and Sauvage, B.: Anthropogenic emissions in Nigeria and implications for atmospheric ozone pollution: A view from space. Atmos. Environ., 99, 32-40, https://doi.org/10.1016/j.atmosenv.2014.09.055, 2014.

Marais, E. A., Silvern, R. F., Vodonos, A., Dupin, E., Bockarie, A. S., Mickley, L. J., and Schwartz, J.: Air Quality and Health Impact of Future Fossil Fuel Use for Electricity Generation and Transport in Africa. Environmental Science and Technology, 53(22), 13524–13534, https://doi.org/10.1021/acs.est.9b04958, 2019.

Marrapu, P., Cheng, Y., Beig, G., Sahu, S., Srinivas, R., and Carmichael, G.R.: Air quality in Delhi during the Commonwealth games. Atmos. Chem. Phys. 14, 10619- 10630, 2014.

Mazzeo, A., Burrow, M., Quinn, A., Marais, E.A., Singh, A., Nganga, D., Gichuru, M.J., and Pope, F.D.: Evaluation of the WRF and CHIMERE models for the simulation of $PM_{2.5}$ in large East African urban conurbations. Atmospheric Chemistry and Physics, 22, 10677-10701, 10.5194/acp-22-10677-2022, 2022.

Nedbor-Gross, R., Henderson, B.H., Perez-Pena, M.P., and Pachon, J.E.: Air quality modeling in Bogota Colombia using local emissions and natural mitigation factor adjustment for re-suspended particulate matter. Atmos. Pollut. Res. 9, 95-104, https://doi.org/10.1016/j.apr.2017.07.004, 2018.

Okimiji, O. P., Techato, K., Simon, J. N., Tope-Ajayi, O. O., Okafor, A. T., Aborisade, M. A., and Phoungthong, K.: Spatial pattern of air pollutant concentrations and their relationship with meteorological parameters in coastal slum settlements of Lagos, Southwestern Nigeria. Atmosphere, 12(11), https://doi.org/10.3390/atmos12111426, 2021.

Owoade, O. K., Fawole, O. G., Olise, F. S., Ogundele, L. T., Olaniyi, H. B., Almeida, M. S., Ho, M. D., and Hopke, P. K.: Characterization and source identification of airborne particulate loadings at receptor site-classes of Lagos Mega-City, Nigeria. Journal of the Air and Waste Management Association, 63(9), 1026–1035, https://doi.org/10.1080/10962247.2013.793627, 2013.

Owoade, O.K., Abiodun, P.O., Omokungbe, O.R., Fawole, O.G., Olise, F.S., Popoola, O.O.M., Jones, R.L., and Hopke, P.K.: Spatial-temporal Variation and Local

Source Identification of Air Pollutants in a Semi-urban Settlement in Nigeria Using Low-cost Sensors. Aerosol Air Qual. Res. 21, 200598, https://doi.org/10.4209/aaqr.200598, 2021.

Pan, S., Choi, Y., Roy, A., and Jeon, W.: Allocating emissions to 4 km and 1 km horizontal spatial resolutions and its impact on simulated NO_x and O_3 in Houston, TX. Atmos. Environ., 164, 398-415, https://doi.org/10.1016/j.atmosenv.2017.06.026, 2017.

Pedruzzi, R., Baek, B. H., Henderson, B. H., Aravanis, N., Pinto, J. A., Araujo, I. B., Nascimento, E. G. S., Reis Junior, N. C., Moreira, D. M., and de Almeida Albuquerque, T. T.: Performance evaluation of a photochemical model using different boundary conditions over the urban and industrialized metropolitan area of Vitória, Brazil. Environmental Science and Pollution Research, 26(16), 16125–16144, https://doi.org/10.1007/s11356-019-04953-1, 2019.

Pedruzzi, R., Andreão, W. L., Baek, B. H., Hudke, A. P., Glotfelty, T. W., Dias de Freitas, E., Martins, J. A., Bowden, J. H., Pinto, J. A., Alonso, M. F., and de Almeida Abuquerque, T.T: Update of land use/land cover and soil texture for Brazil: Impact on WRF modeling results over São Paulo. Atmos. Environ., 268, 118760, https://doi.org/10.1016/j.atmosenv.2021.118760, 2022.

Qiao, X., Tang, Y., Hu, J., Zhang, S., Li, J., Kota, S. H., Wu, L., Gao, H., Zhang, H., and Ying, Q.: Modeling dry and wet deposition of sulfate, nitrate, and ammonium ions in Jiuzhaigou National Nature Reserve, China using a source-oriented CMAQ model: Part I. Base case model results. Sci. Total Environ., 532: 831-839, 2015.

Qiao, X., Guo, H., Tang, Y., Wang, P., Deng, W., Zhao, X., Hu, J., Ying, Q., and Zhang, H.: Local and regional contributions to fine particulate matter in the 18 cities of Sichuan Basin, southwestern China. Atmospheric Chemistry and Physics, 19(9), 5791-5803, https://doi.org/10.5194/acp-19-5791-2019, 2019.

Reis, S., Liška, T., Vieno, M., Carnell, E.J., Beck, R., Clemens, T., Dragosits, U., Tomlinson, S.J., Leaver, D., and Heal, M.R.: The influence of residential and workday population mobility on exposure to air pollution in the UK. Environ. Int. 121, 803-813, https://doi.org/10.1016/j.envint.2018.10.005, 2018.

Rizwan, S. A., Nongkynrih, B., and Gupta, S. K.: Air pollution in Delhi: its magnitude and effects on health. Indian journal of community medicine: official publication of Indian Association of Preventive & Social Medicine, 38(1), 4, 2013.

Shen, J., Zhao, Q., Cheng, Z., Huo, J., Zhu, W., Zhang, Y., Duan, Y., Wang, X., Antony Chen, L. W., and Fu, Q.: Evolution of source contributions during heavy fine particulate matter ($PM_{2.5}$) pollution episodes in eastern China through online measurements. Atmos. Environ., 232, https://doi.org/10.1016/j.atmosenv.2020.117569, 2020.

Shi, Z., Li, J., Huang, L., Wang, P., Wu, L., Ying, Q., Zhang, H., Lu, L., Liu, X., Liao, H., and Hu, J.: Source apportionment of fine particulate matter in China in 2013 using a source-oriented chemical transport model. Science of the Total Environment, 601-602, 1476-1487, https://doi.org/10.1016/j.scitotenv.2017.06.019, 2017.

Sulaymon, I. D., Mei, X., Yang, S., Chen, S., Zhang, Y., Hopke, P. K., Schauer, J. J., and Zhang, Y.: $PM_{2.5}$ in Abuja, Nigeria: Chemical characterization, source apportionment, temporal variations, transport pathways and the health risks assessment. Atmospheric Research, 237, https://doi.org/10.1016/j.atmosres.2019.104833, 2020.

Sulaymon, I. D., Zhang, Y., Hopke, P. K., Hu, J., Zhang, Y., Li, L., Mei, X., Gong, K., Shi, Z., Zhao, B., and Zhao, F.: Persistent high $PM_{2.5}$ pollution driven by unfavorable meteorological conditions during the COVID-19 lockdown period in the Beijing-Tianjin-Hebei region, China. Environmental Research, 198. https://doi.org/10.1016/j.envres.2021.111186, 2021a.

Sulaymon, I. D., Zhang, Y., Hu, J., Hopke, P. K., Zhang, Y., Zhao, B., Xing, J., Li, L., and Mei, X.: Evaluation of regional transport of $PM_{2.5}$ during severe atmospheric pollution episodes in the western Yangtze River Delta, China. Journal of Environmental Management, 293, https://doi.org/10.1016/j.jenvman.2021.112827, 2021b.

Sulaymon, I. D., Zhang, Y., Hopke, P. K., Zhang, Y., Hua, J., and Mei, X.: COVID-19 pandemic in Wuhan: Ambient air quality and the relationships between criteria air pollutants and meteorological variables before, during, and after lockdown. Atmospheric Research, 250, https://doi.org/10.1016/j.atmosres.2020.105362, 2021c.

Sulaymon, I. D., Zhang, Y., Hopke, P. K., Hu, J., Rupakheti, D., Xie, X., Zhang, Y., Ajibade, F. O., Hua, J., and She, Y.: Influence of transboundary air pollution and meteorology on air quality in three major cities of Anhui Province, China. Journal of Cleaner Production, 129641, https://doi.org/10.1016/j.jclepro.2021.129641, 2021d.

Tao, H., Xing, J., Zhou, H., Pleim, J., Ran, L., Chang, X., Wang, S., Chen, F., Zheng, H., and Li, J.: Impacts of improved modeling resolution on the simulation of meteorology, air quality, and human exposure to $PM_{2.5}$, O_3 in Beijing, China. Journal of Cleaner Production, 243, https://doi.org/10.1016/j.jclepro.2019.118574, 2020.

Tiwari, S., Thomas, A., Rao, P., Chate, D. M., Soni, V. K., Singh, S., Ghude, S. D., Singh, D., and Hopke, P. K.: Pollution concentrations in Delhi India during winter 2015-2016: A case study of an odd-even vehicle strategy. Atmos. Pollut. Res., 9, 1137-1145, 2019.

Wang, P., Ying, Q., Zhang, H., Hu, J., Lin, Y., and Mao, H.: Source apportionment of secondary organic aerosol in China using a regional source-oriented chemical transport model and two emission inventories. Environmental Pollution, 237, 756-766, https://doi.org/10.1016/j.envpol.2017.10.122, 2018.

Wang, P., Chen, K., Zhu, S., Wang, P., and Zhang, H.: Severe air pollution events not avoided by reduced anthropogenic activities during COVID-19 outbreak. Resources, Conservation and Recycling, 158, https://doi.org/10.1016/j.resconrec.2020.104814, 2020.

Wang, P., Wang, P., Chen, K., Du, J., and Zhang, H.: Ground-level ozone simulation using ensemble WRF/Chem predictions over the Southeast United States. Chemosphere, 287, https://doi.org/10.1016/j.chemosphere.2021.132428, 2021a.

Wang, X., Li, L., Gong, K., Mao, J., Hu, J., Li, J., Liu, Z., Liao, H., Qiu, W., Yu, Y., Dong, H., Guo, S., Hu, M., Zeng, L., and Zhang, Y.: Modelling air quality during the EXPLORE-YRD campaign - Part I. Model performance evaluation and impacts

of meteorological inputs and grid resolutions. Atmos. Environ., 246, https://doi.org/10.1016/j.atmosenv.2020.118131, 2021b.
WHO. WHO Air Quality Guidelines Global Update.: Particulate Matter, Ozone, Nitrogen Dioxide and Sulphur Dioxide; World Health Organization Regional Office for Europe. World Health Organization, Copenhagen, Denmark, 2005.
Wiedinmyer, C., Akagi, S., Yokelson, R. J., Emmons, L., Al-Saadi, J., Orlando, J., and Soja, A.: The Fire INventory from NCAR (FINN): A high resolution global model to estimate the emissions from open burning. Geoscientific Model Devel., 4 (3), 625, 2011.
World Health Organization.: WHO Global Air Quality Guidelines: Particulate Matter ($PM_{2.5}$ and PM_{10}), Ozone, Nitrogen Dioxide, Sulfur Dioxide and Carbon Monoxide. World Health Organization. Available at: https://apps.who.int/iris/handle/10665/345329, 2021.
Yan, D., Lei, Y., Shi, Y., Zhu, Q., Li, L., and Zhang, Z.: Evolution of the spatiotemporal pattern of $PM_{2.5}$ concentrations in China - A case study from the Beijing-Tianjin-Hebei region. Atmos. Environ., 183, 225–233, https://doi.org/10.1016/j.atmosenv.2018.03.041, 2018.
Ye, F., Rupakheti, D., Huang, L., T, Nishanth., MK, S.K., Li, L., KT, V., Hu, J.: Integrated process analysis retrieval of changes in ground-level ozone and fine particulate matter during the COVID-19 outbreak in the coastal city of Kannur, India. Environmental Pollution, 307, https://doi.org/10.1016/j.envpol.2022.119468, 2022.
Ying, Q. and Kleeman, M.J.: Source contributions to the regional distribution of secondary particulate matter in California. Atmos. Environ., 40, 736-752, 2006.
Ying, Q., Wu, L., and Zhang, H.: Local and inter-regional contributions to $PM_{2.5}$ nitrate and sulfate in China. Atmos. Environ., 94, 582-592, 2014.
Ying, Q., Li, J., and Kota, S.H.: Significant contributions of isoprene to summertime secondary organic aerosol in eastern United States. Environ. Sci. Technol., 49, 7834-7842, 2015.
Yu, Y., Xu, H., Jiang, Y., Chen, F., Cui, X., He, J., and Liu, D.: A modeling study of $PM_{2.5}$ transboundary during a winter severe haze episode in southern Yangtze River Delta, China. Atmos. Res., 248, 105159, 2021.
Zhang, H., Li, J., Ying, Q., Guven, B.B., and Olaguer, E.P.: Source apportionment of formaldehyde during TexAQS 2006 using a source-oriented chemical transport model. J. Geophys. Res. Atmos., 118, 1525-1535, 2013.
Zhang, H., Hu, J., Kleeman, M., and Ying, Q.: Source apportionment of sulfate and nitrate particulate matter in the Eastern United States and effectiveness of emission control programs. Sci. Total Environ. 490, 171-181, 2014.
Zhang, H., Wang, Y., Hu, J., Ying, Q., and Hu, X.: Relationships between meteorological parameters and criteria air pollutants in three megacities in China. Environ. Res., 140, 242-254, 2015.
Zhang, H., Cheng, S., Yao, S., Wang, X., and Zhang, J.: Multiple perspectives for modeling regional $PM_{2.5}$ transport across cities in the Beijing-Tianjin-Hebei region during haze episodes. Atmos. Environ., 212, 22-35, 2019.
Zhang, Q., Ma, Q., Zhao, B., Liu, X., Wang, Y., Jia, B., and Zhang, X.: Winter haze over North China Plain from 2009 to 2016: Influence of emission and

meteorology. Environmental Pollution, https://doi.org/10.1016/j.envpol.2018.08.019, 2018.

Zhao, X., Wang, G., Wang, S., Zhao, N., Zhang, M., and Yue, W.: Impacts of COVID-19 on air quality in mid-eastern China: An insight into meteorology and emissions. Atmos. Environ., 266, https://doi.org/10.1016/j.atmosenv.2021.118750, 2021.

Supplementary Material for

Modelling $PM_{2.5}$ during severe atmospheric pollution episode in Lagos, Nigeria: Spatiotemporal variations, source apportionment, and meteorological influences

Ishaq Dimeji Sulaymon[a*], Yuanxun Zhang[b,c], Philip K. Hopke[d,e], Fei Ye[a], Kangjia Gong[a], Jianjiong Mao[a], Jianlin Hu[a*]

[a] *Jiangsu Key Laboratory of Atmospheric Environment Monitoring and Pollution Control, Collaborative Innovation Center of Atmospheric Environment and Equipment Technology, School of Environmental Science and Engineering, Nanjing University of Information Science & Technology, Nanjing, 210044, China*

[b] *College of Resources and Environment, University of Chinese Academy of Sciences, Beijing 100049, China*

[c] *CAS Center for Excellence in Regional Atmospheric Environment, Chinese Academy of Sciences, Xiamen, 361021, China*

[d] *Center for Air Resources Engineering and Science, Clarkson University, Potsdam, NY 13699, USA*

[e] *Department of Public Health Sciences, University of Rochester School of Medicine and Dentistry, Rochester, NY 14642, USA*

[*] Corresponding author. *E-mail address:* sulaymondimeji@nuist.edu.cn; jianlinhu@nuist.edu.cn

Table S1. The major physics options and the schemes used in the WRF model.

Physics option	Scheme
Microphysics	Thompson scheme
Shortwave radiation	RRTMG scheme
Longwave radiation	RRTMG scheme
Surface layer	Revised MM5 Monin-Obukhov scheme
Land surface	Unified Noah land-surface scheme
Planetary boundary layer	YSU scheme
Cumulus parameterization	Grell-Freitas ensemble scheme

Table S2. Concentration range under different $PM_{2.5}$ pollution levels.

Levels	Clean	Slightly polluted	Moderately polluted	Heavily polluted	Severely polluted
Concentration (μg/m^3)	$PM_{2.5}$<35	35≤ $PM_{2.5}$<75	75≤ $PM_{2.5}$<115	115≤ $PM_{2.5}$<150	150≤ $PM_{2.5}$

Table S3. Statistical results of $PM_{2.5}$ under different pollution levels in Lagos during January 2021.

	Clean (2 days)		Slight (12 days)		Moderate (10 days)		Heavy (5 days)		Severe (2 days)	
	Obs.	Sim.	Obs.	Sim.	Obs.	Sim.	Obs.	Sim.	Obs.	Sim.
Minimum	15.7	11.9	44.3	48.8	72.5	79.1	121.7	117.4	161.8	167.3
Maximum	23.7	17.3	76.7	72.4	109.5	107.0	148.2	143.9	214.6	198.6
Mean	19.7	14.6	60.4	62.7	88.7	92.5	134.7	135.9	188.2	182.9

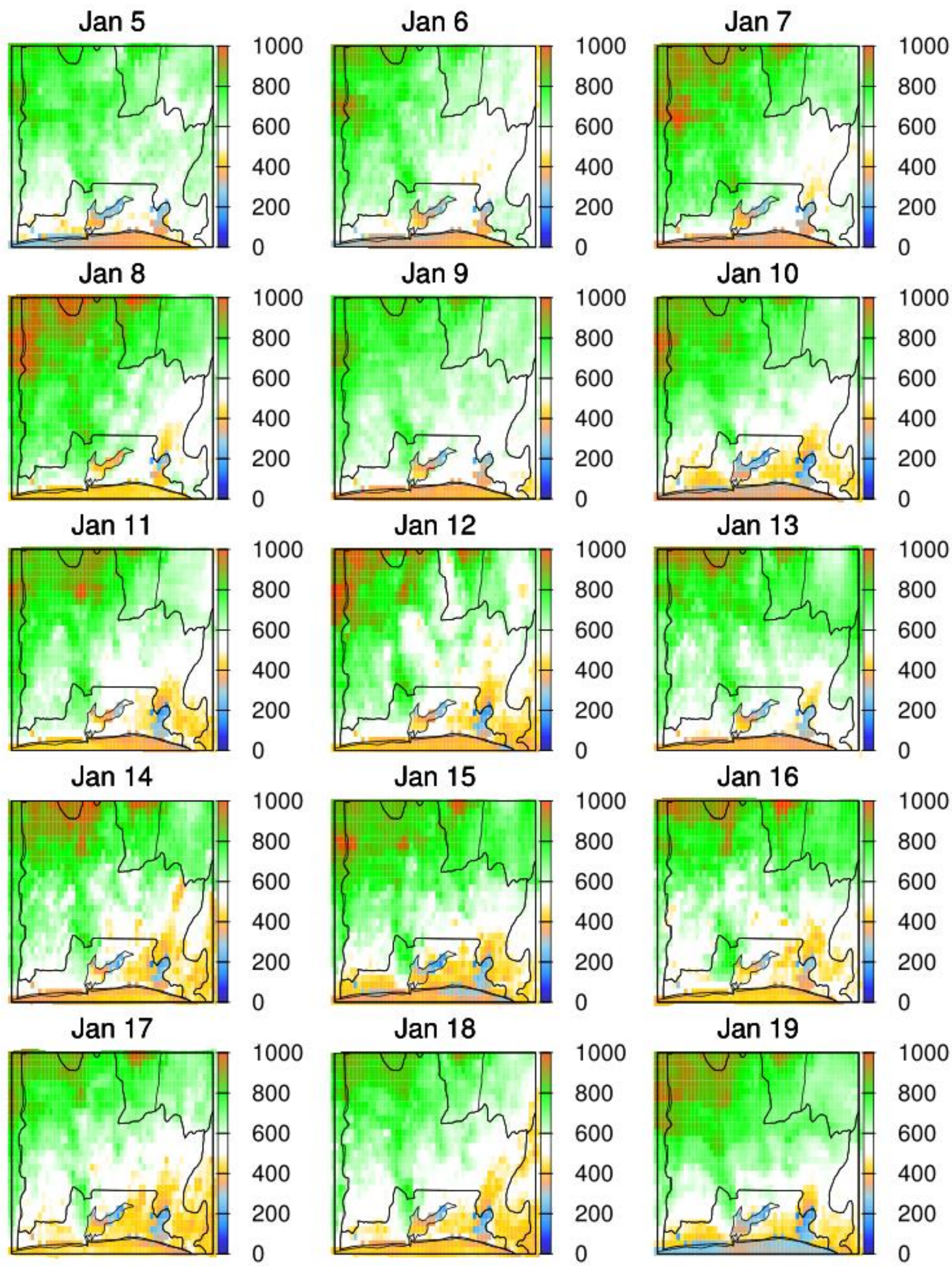

Figure S1. Spatial distributions of the predicted planetary boundary layer height (PBLH) in Lagos during the atmospheric pollution episode. Units are m.

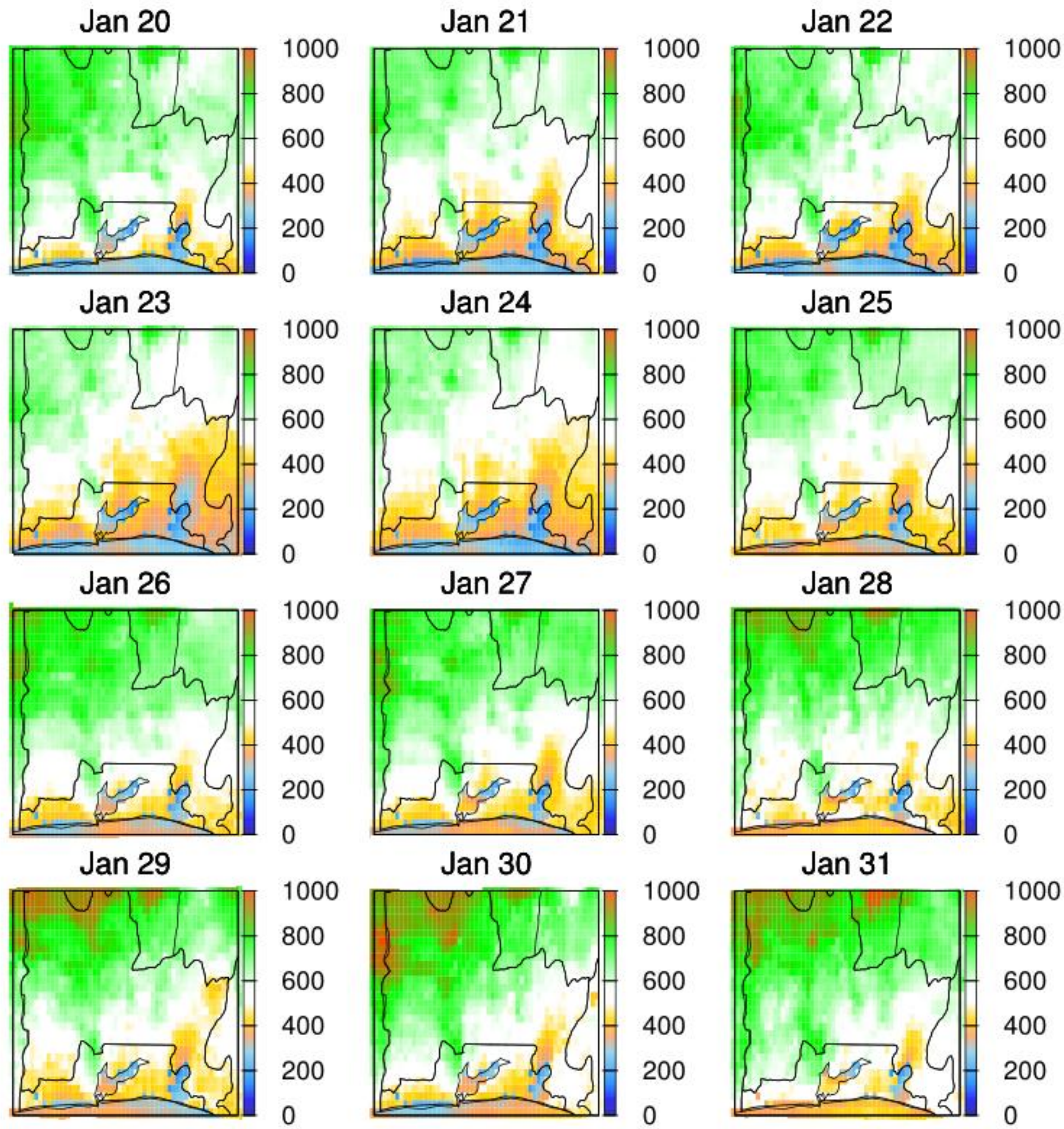

Figure S1. (continued).

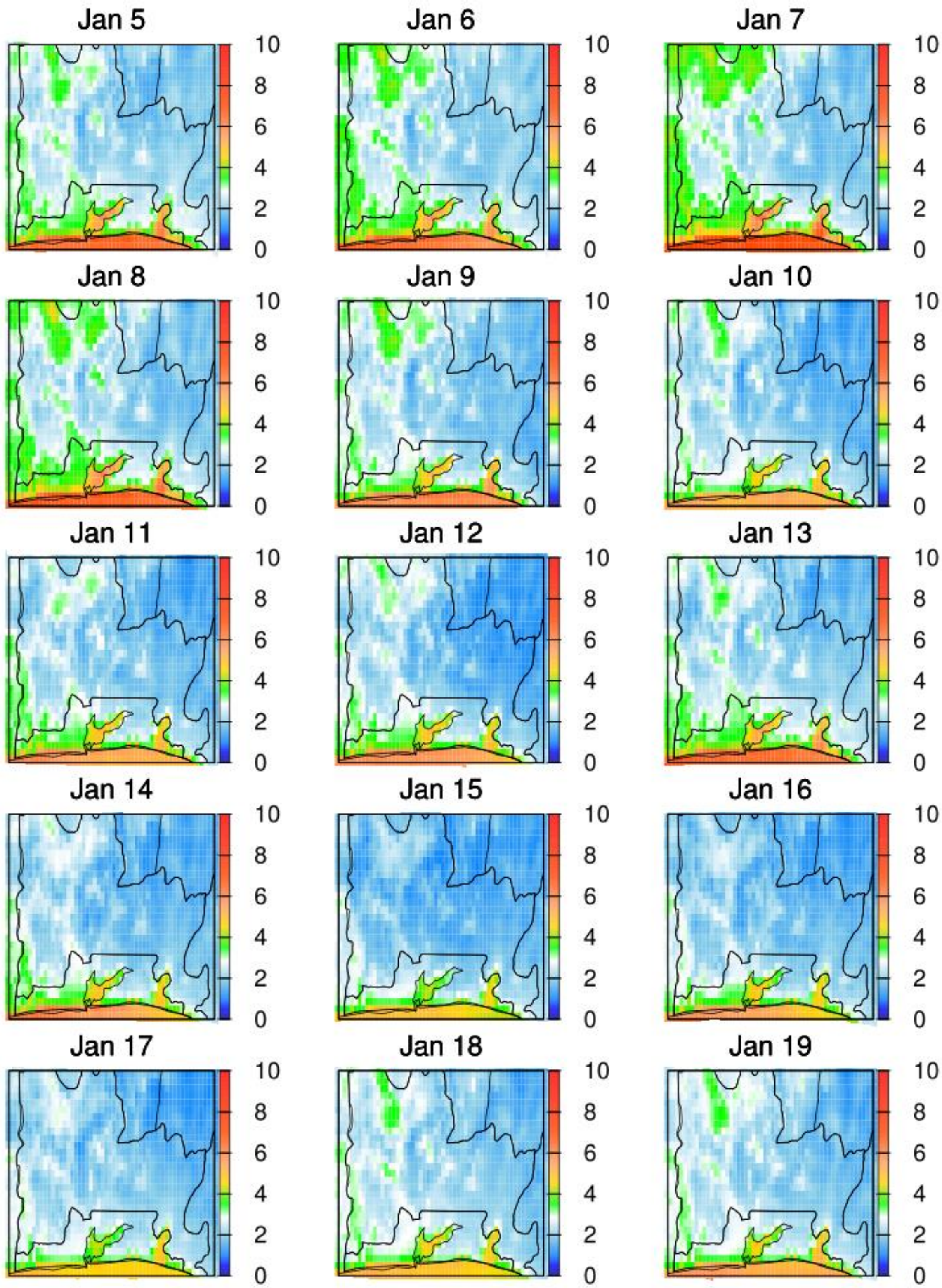

Figure S2. Spatial distributions of the predicted wind speed at 10 m (WS10) in Lagos during the atmospheric pollution episode. Units are m/s.

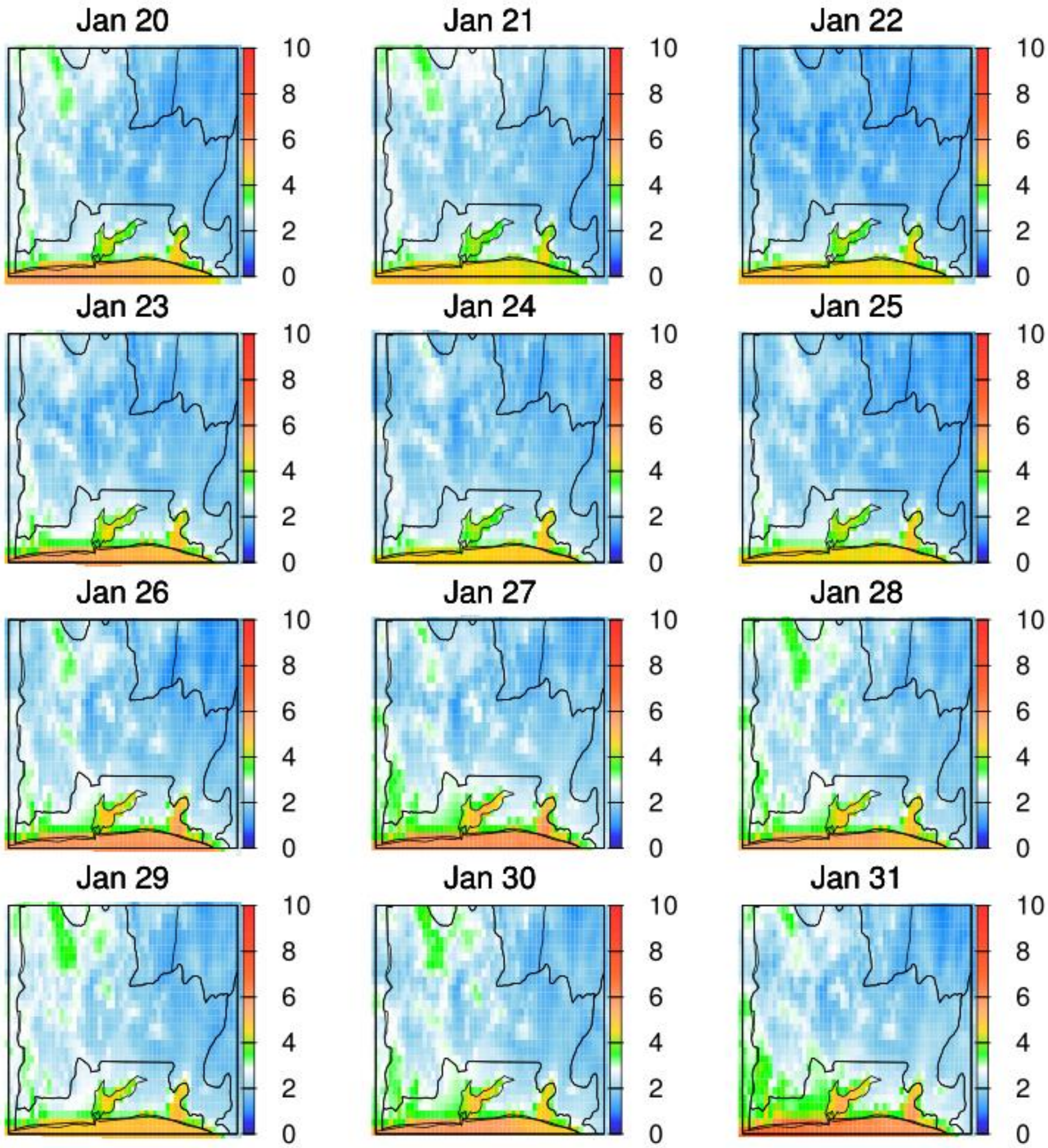

Figure S2. (continued).

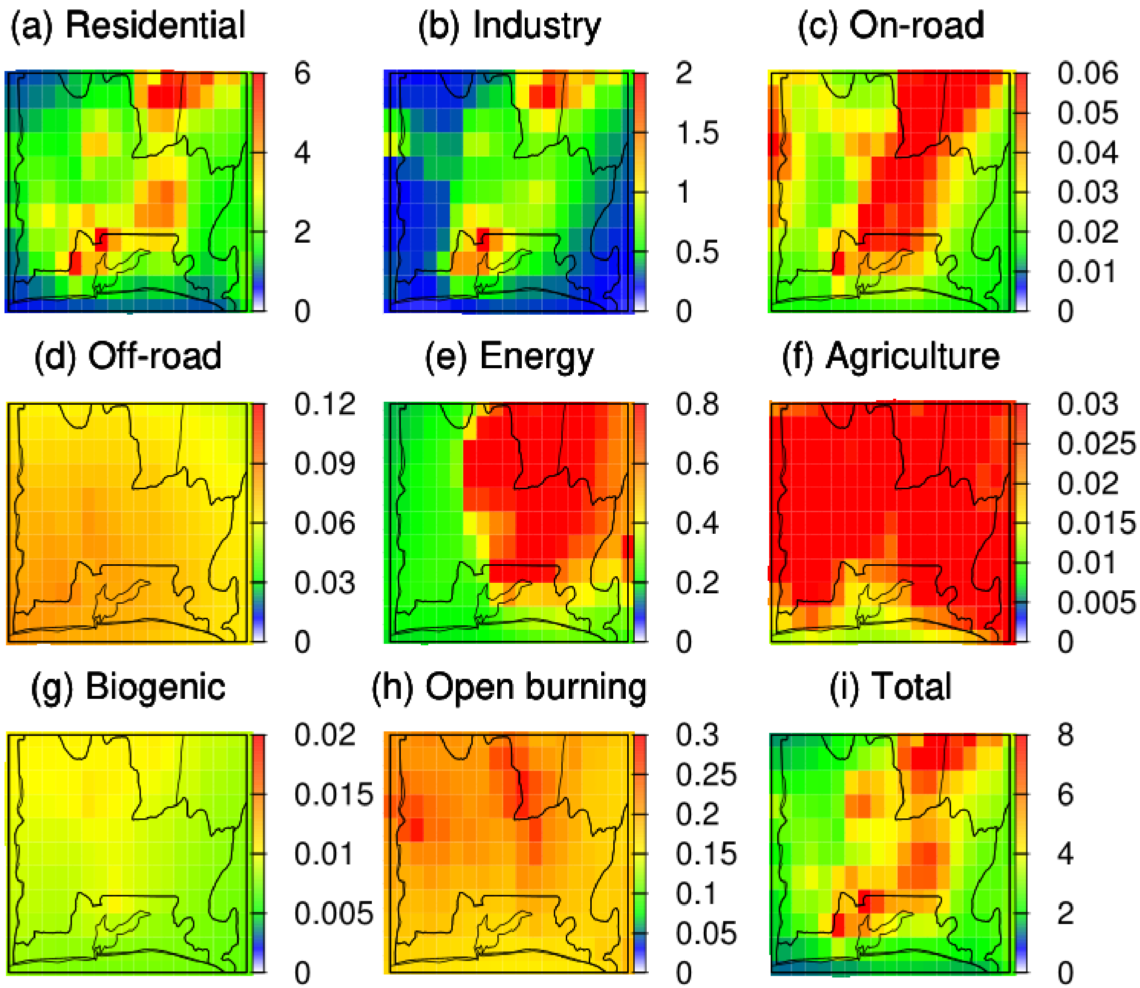

Figure S3. Source apportionment of SO_4^{2-} from (a) residential, (b) industry, (c) on-road, (d) off-road, (e) energy, (f) agriculture, (g) biogenic, and (h) open burning during the atmospheric pollution episode. Units are μg/m^3.

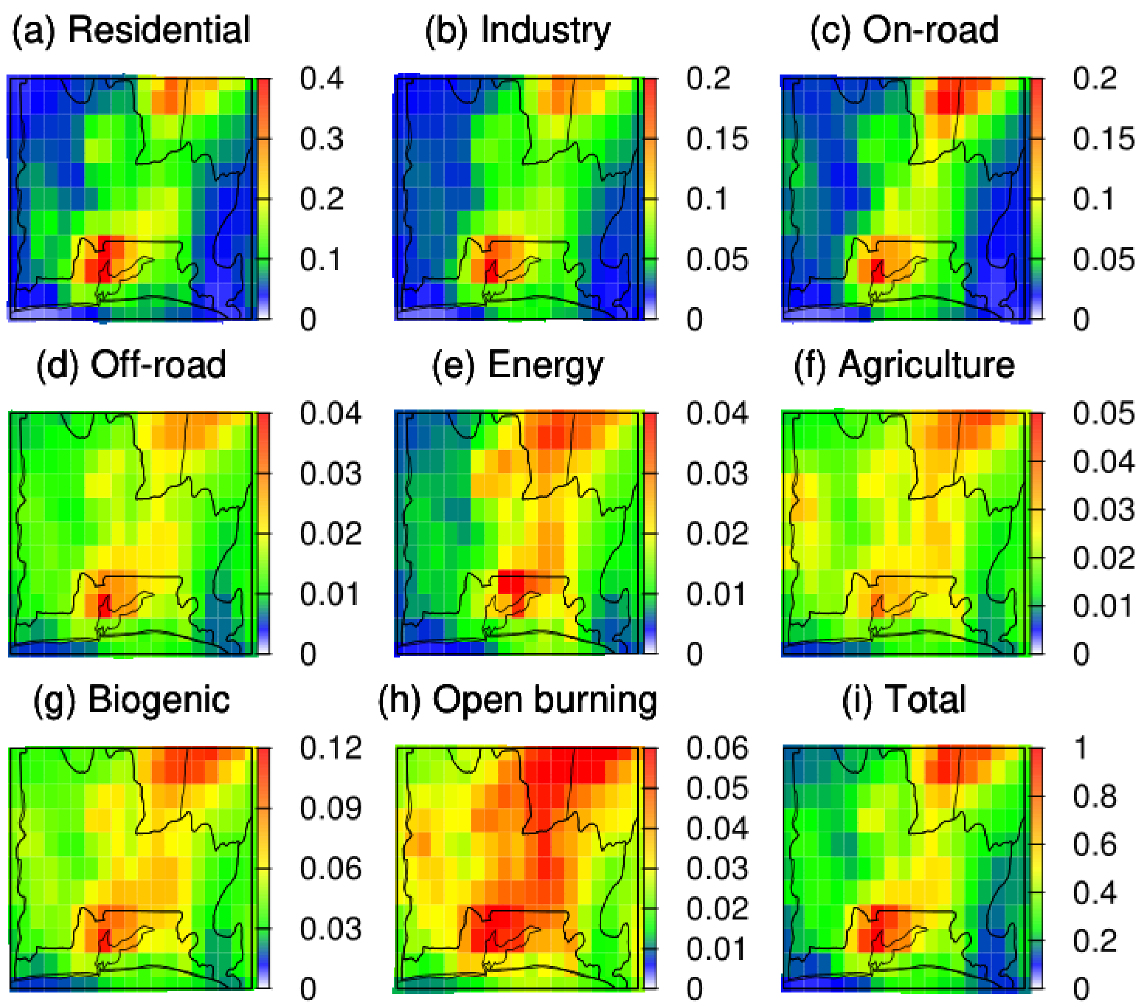

Figure S4. Source apportionment of NO_3^- from (a) residential, (b) industry, (c) on-road, (d) off-road, (e) energy, (f) agriculture, (g) biogenic, and (h) open burning during the atmospheric pollution episode. Units are μg/m^3.

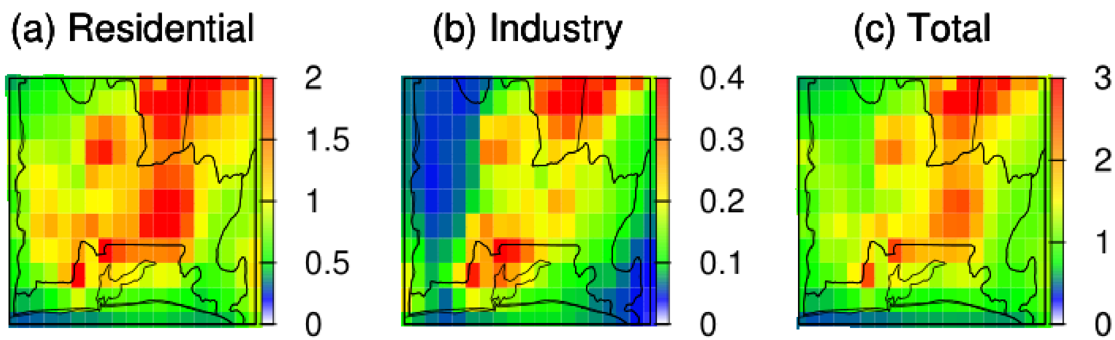

Figure S5. Source apportionment of NH_4^+ from (a) residential, (b) industry, (c) on-road, (d) off-road, (e) energy, (f) agriculture, (g) biogenic, and (h) open burning during the atmospheric pollution episode. Units are μg/m^3.

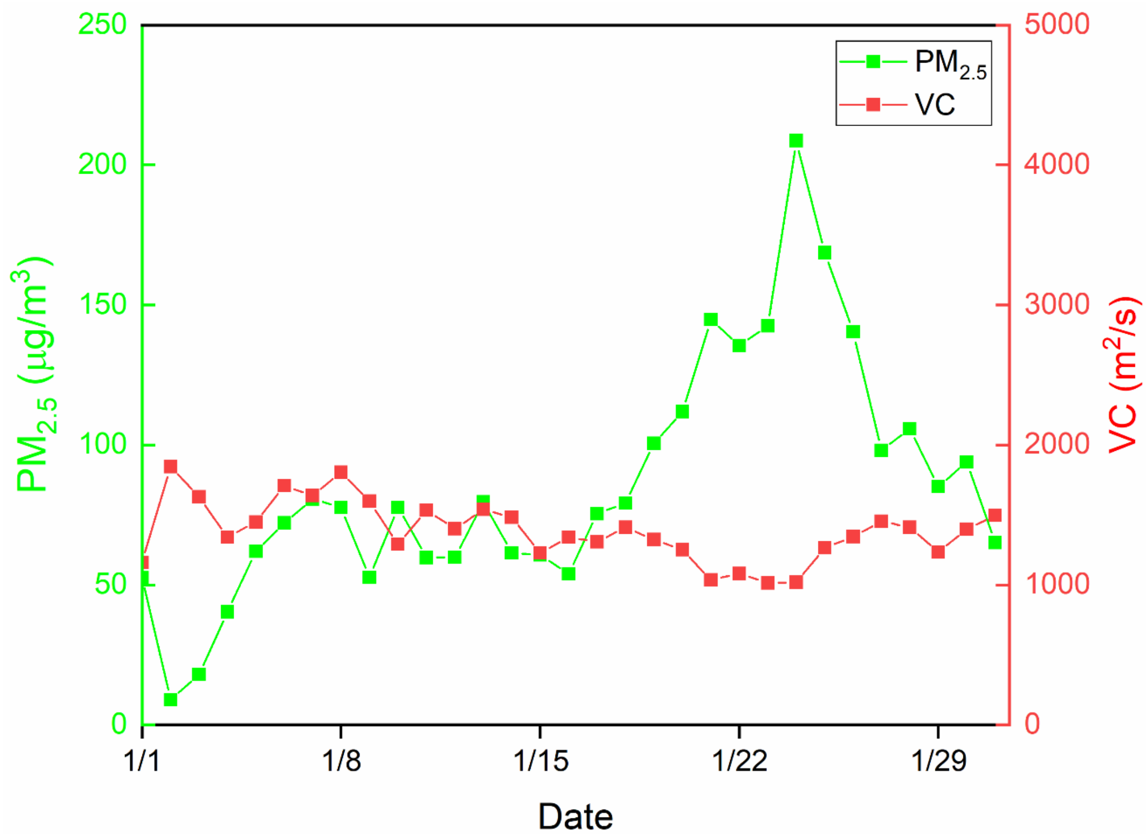

Figure S6. Temporal variations of $PM_{2.5}$ ($\mu g/m^3$) and VC (m^2/s) in Lagos during January 2021.